

MTENG-6490.pdf

By Sri Atmaja Rosyidi

WORD COUNT

11212

TIME SUBMITTED

14-MAY-2018 11:33AM

PAPER ID

37193925

Wavelet Spectrogram Analysis of Surface Wave Technique for In-situ Pavement Stiffness Measurement

--Manuscript Draft--

Manuscript Number:	MTENG-6490R2
Full Title:	Wavelet Spectrogram Analysis of Surface Wave Technique for In-situ Pavement Stiffness Measurement
Article Type:	Technical Paper
Abstract:	<p>Accurate, quick, non-destructive in-situ tests for measuring pavement stiffness, or elastic modulus, are an increasingly important element in pavement management systems. This is due to the increasing number of aged road networks and the limited budget allocated by the government for pavement monitoring and maintenance. This paper aims to propose a new wavelet-spectrogram analysis of surface wave (WSSW) technique for a non-destructive testing and in situ measurement of pavement surface layers. The proposed technique was developed based on the spectral-analysis of surface wave (SASW) and modified data analysis of the ultrasonic-surface-wave (USW) methods. This technique utilizes two receivers to detect and record the signals of the surface wave propagating on a pavement surface. In wavelet analysis, the received signals are transformed into a time-frequency domain and displayed in a spectrogram. The spectrogram was generated based on the mother wavelet of Gaussian derivative (GoD). A wavelet filtration technique was also used in the time-frequency spectrogram to diminish the effect of the noise signal recorded during field measurement. The unwrapped phase of a different spectrum was generated from a selected wave-energy in the spectrogram to obtain a phase velocity; this is done through a linear regression analysis for calculating the value of the slope of a phase velocity. The elastic modulus of pavement surface layer can be obtained via a linear relationship of assumed density, measured phase velocity, and assumed Poisson ratio of pavement materials. The results can be used to show that the proposed technique can be of practical use for in situ elastic modulus measurement on flexible and rigid pavements. It can also be used to determine any changes that might occur in the stiffness pavement surface layer.</p>

8
1 **Wavelet-Spectrogram Analysis of Surface Wave Technique for**
2 **In-Situ Pavement Stiffness Measurement**

49
4 Sri Atmaja P. Rosyidi, Ph.D., P.Eng.

4
5 Associate Professor, Department of Civil Engineering, Universitas
6 Muhammadiyah Yogyakarta, Bantul, 55183, Yogyakarta, Indonesia, Email:
7 atmaja_sri@umy.ac.id

9 Nur Izzi Md. Yusoff, Ph.D.

4
10 Senior Lecturer, Department of Civil and Structural Engineering, Universiti
11 Kebangsaan Malaysia, 43600 Bandar Baru Bangi, Malaysia Email:
12 izzi@ukm.edu.my

14 **ABSTRACT**

15 Accurate, quick, non-destructive in-situ tests for measuring pavement stiffness, or
16 elastic modulus, is an increasingly important element in pavement management
17 systems. This is 5 due to the increasing number of aged road networks and the
18 limited budget allocated by the government for pavement monitoring and
19 maintenance. This paper aims to propose a new 8 wavelet-spectrogram analysis of
20 surface wave (WSSW) technique for a non-destructive testing and in situ
21 measurement of pavement surface layers. The proposed technique was developed
22 based on the 14 spectral-analysis of surface wave (SASW) and modified data analysis
23 of the ultrasonic-surface-wave (USW) methods. This technique utilizes two
24 receivers to detect and record the signals of the surface wave propagating on a
25 pavement surface. In wavelet analysis, the received signals 10 are transformed into a

26 time-frequency domain and displayed in a spectrogram. The spectrogram was
27 generated based on the mother wavelet of Gaussian derivative (GoD). A wavelet
28 filtration technique was also used in the time-frequency spectrogram to diminish
29 the effect of the noise signal recorded during field measurement. The unwrapped
30 phase of a different spectrum was generated from a selected wave-energy in the
31 spectrogram to obtain a phase velocity; this is done through a linear regression
32 analysis for calculating the value of the slope of a phase velocity. The elastic
33 modulus of pavement surface layer can be obtained via a linear relationship of
34 assumed density, measured phase velocity, and assumed Poisson ratio of pavement
35 materials. The results can be used to show that the proposed technique can be of
36 practical use for in situ elastic modulus measurement on flexible and rigid
37 pavements. It can also be used to determine any changes that might occur in the
38 stiffness pavement surface layer.

39 **Keywords:** elastic modulus, pavement surface layer; surface wave techniques,
40 wavelet analysis

41

42 INTRODUCTION

43

44 SASW is one of the frequently used non-destructive testing (NDT) methods for
45 assessing the material strength of pavement structures. This method uses the
46 dispersive characteristics of seismic surface wave to determine the stiffness profile
47 of shear wave velocity which corresponds with the elastic modulus of a pavement
48 layer. This method comprises three steps of data analysis, i.e., (1) recording the
49 signals and analyzing its spectrum based on the measured seismic waves
50 propagation, (2) generating experimental dispersion curves from the results of

51 phase velocity analysis, and (3) inverting the experimental dispersion curves to
52 generate a shear wave velocity profile. Researchers have conducted studies on the
53 various ways the SASW method was used. Amongst them are the use of SASW
54 for soil characterization (Stokoe et. al. 1994, Kim et. al. 2001); evaluation of
55 dynamic soil properties (Rosyidi and Taha 2012); pavement investigation (Rosyidi
56 et. al. 2007, Yusoff et. al. 2013, Rosyidi, 2017); and measuring of the stiffness of
57 asphaltic pavements (Shirazi et al. 2009, Hazra and Kumar 2014).

58

59 In order to generate a stiffness profile, or shear wave velocity, of a pavement, an
60 advanced mathematical approach was used to invert the SASW method. Several
61 elastic stress wave theories for solids have been developed to derive theoretical
62 dispersion curves in the attempt to produce a reliable inversion analysis. Among
63 them are the transfer and dynamic stiffness matrix, which use plane-wave
64 approximations and assume that the pavement system comprises profile layers with
65 homogeneous and isotropic properties; generalized reflection-transmission
66 coefficient; finite element; and finite difference methods. These inversion
67 processes utilized existing information of model parameters in an initial profile
68 consisting of a set of horizontal homogeneous layers with constant stiffness in the
69 horizontal direction overlaying a half-space. Layer thickness, stress wave
70 velocities (shear and compression wave), Poisson's ratio of the material and density
71 are assigned to each layer of the profile. A change in the Poisson's ratio and
72 density of the material has a negligibly small effect on the calculated dispersion
73 curve (Tokimatsu et al., 1992). This initial profile is then used as a basis for
74 calculating a theoretical dispersion curve by using one of the elastic stress wave
75 theories. Once a theoretical dispersion curve has been obtained, the inversion

76 method is iteratively implemented by comparing the theoretical curve with the
77 experimental data. This comparison is done by calculating the error between the
78 theoretical and experimental data, such as the root mean square error. If the match
79 is not acceptable or if the error of the dispersion curves is large, the initial profile is
80 updated and the new profile is used to produce a new theoretical dispersion curve.
81 The process is iterated until both curves match, and only matched theoretical curve
82 are considered as a real profile. However, in the case of an irregular profile such as
83 pavements, the inversion process becomes more difficult and requires extended
84 data processing time. Many researchers have elaborated on the difficulties they
85 encountered when applying the SASW method on pavement profile. Al-Hunaidi
86 (1992), Tokimatsu et. al. (1992), Ganji et. al. (1998), Ryden et. al. (2004) reported
87 that most of the difficulties are due to the effect of higher modes stress wave
88 propagation.

89
90 The conventional stress wave propagation analysis in the SASW inversion method
91 is not capable of directly distinguishing between the fundamental and the higher
92 modes that occur in a pavement system. It is also unable to clearly observe the
93 stress waves propagation superposition modes if it is only based on the field
94 configuration and receiver locations. This effect, which is also known as apparent
95 phase velocity, varies with distance and has an effect on receivers position for data
96 analysis and the fundamental and higher- modes superposition for the inversion
97 analysis. Ryden et. al. (2004) proposed a new approach for conducting seismic
98 testing on pavements. This method is able to distinguish stress wave propagation
99 modes, thereby solving some of the difficulties commonly encountered in
100 pavement testing. They used a multichannel simulation with one receiver (MSOR)

101 method, which was developed from the concept of multichannel analysis of surface
102 wave (MASW) which typically requires a minimum of 48 receivers, to gather data.
103 Results show that the dispersion of stress waves in a pavement profile for a
104 frequency of between 50 to 3,000 Hz cannot be represented with only one average
105 dispersion curve. The high frequency range of the dispersion curve is matched with
106 theoretical Lamb waves in a free plate, while the lower frequencies are matched
107 with several branches of dispersion curves which correspond with each layer of the
108 varying stiffness in the pavement profile. However, due to the complexity in
109 interpreting surface wave as well as the tedious and complicated data analysis, the
110 MASW and MSOR methods are not widely used in structural pavement
111 assessment.

112

113 There is an urgent need to develop a quick, practical, accurate, cost-efficient, non-
114 intrusive test for evaluating pavement systems since pavement maintenance and
115 management is a cumulatively complex process due to the increasing number of
116 aging roads and the limited budget allocated by the government. Additionally, for
117 practical and functional purposes, pavement engineers need to be able to do rapid
118 assessment and reasonably simple analysis to measure the stiffness of pavement
119 surface layer.

120

121 This paper introduces a new technique for measuring surface wave which uses a
122 combination of continuous wavelet transform and a simple formulation of phase
123 data, phase velocity, and elastic stiffness relationships to determine the surface
124 stiffness of a pavement structure. This technique is known as the wavelet-
125 spectrogram analysis of surface wave (WSSW). A continuous wavelet transforms

126 (CWT) is used to decompose the received seismic signals and to identify and
127 enhance the phase information from the time-frequency spectrogram. The
128 technique is utilized to improve the phase data obtained from the signals. Seismic
129 data in the conventional SASW method is usually processed and analyzed in
130 frequency domain by using the fast Fourier transforms (FFT). However, since
131 Fourier transform works by utilizing any arbitrary periodic sinusoidal function of
132 time, the analysis is not appropriate for interpreting the spectral characteristics for
133 non-stationary signals (Rosyidi et.al. 2009). Wavelet is being used more
134 frequently as an effective analysis for seismic signals in the time dimension and for
135 localizing various their spectral events. A time-frequency spectrogram can be
136 generated in wavelet analysis to examine the signals in the time and frequency
137 domains simultaneously. Therefore, the translation and scaling process in wavelet
138 analysis is of particular use for measuring the influence of the varying seismic
139 wave modes and identifying some of the modes in the time domain. Wavelet
140 analysis also allows for a more stable computation of phase velocity in comparison
141 to the phase velocity obtained by using the time-difference method which is
142 commonly employed in traditional SASW. Gucunski and Shokouhi (2005) asserted
143 that CWT analysis can be used to identify the cavities in media sub-surface, i.e.
144 the pavement. It is also capable of differentiating between the characteristics of
145 layer dipping and interface layers when there is an extreme change in stiffness.

146

147 This paper describes the simple procedure of using phase data from wavelet
148 analysis and material properties to obtain the elastic modulus of pavement surface
149 layer without utilizing any complex inversion algorithms. It then presents the
150 typical results from some case studies which were conducted to evaluate the

151 asphalt concrete (AC) layer of pavement structurez at two different locations, i.e.,
152 Purwakarta national highway network, Indonesia and road pavement in Bandar
153 Baru Bangi, Malaysia. Several comparative tests of the WSSW measurement were
154 also conducted on rigid pavements in Yogyakarta, Indonesia.

155

3 156 CONTINUOUS WAVELET TRANSFORM

157 Continuous wavelet transform (CWT) is an interactive signal processing tool used
158 to analyze the time and frequency characteristics of nonstationary seismic signals.
159 It has been variously employed to analyze data in soil and geotechnical
160 investigations (Rosyidi et. al. 2009) and in geophysical methods (Foufoula-
161 Georgiou and Kumar 1995). CWT compares signals with another version of
162 wavelet function. Wavelets compress or stretch in such a way that the time
163 component changes with frequency. The wavelet functions are manipulated in a
164 translation process where the function moves along the time domain and in a
165 dilation process where the wavelet spreads out. When the time domain increases or
166 decreases, the frequency component of the wavelet changed into high or low
167 frequency, respectively. Consequently, as the frequency resolution increases, the
168 time resolution decreases, and vice versa. The ability of CWT to construct a time-
169 frequency resolution generated by wavelet analysis is very suitable for non-
170 stationary seismic analysis.

171

172 A wavelet is expressed as a function of $\psi(t) \in L^2(\mathcal{R})$ and, by dilating and
173 translating the wavelet $\psi(t)$, it is possible to mathematically define a wavelet
174 function as:

$$175 \quad \psi_{\sigma,\tau}(\tau) = \frac{1}{\sqrt{\sigma}} \psi\left(\frac{t-\tau}{\sigma}\right) \quad (1)$$

176 where σ is dilation parameter (it is also referred to as a scale) and τ is translation
 177 parameter ($\sigma, \tau \in \Re$ and $\sigma \neq 0$). The wavelet has varying basic wavelet shapes
 178 which are utilized in seismic data analysis. These shapes are known as mother
 179 wavelet, i.e., Gaussian, Daubechies Haar, Meyer, Morlet, Symlets, Paul,
 180 Biorthogonal and Mexican Hat, which dilate and translate the versions of the
 181 derived mother wavelet which are then used in wavelet analysis. The selection of
 182 a suitable mother wavelet in a particular analysis is based on the waveforms of
 183 seismic signals.

184

185 CWT can be written and derived from the ³⁴ family wavelets $\Psi_{\sigma,\tau}(t)$ with a signal $f(t)$
 186 and is expressed by the following equation:

$$187 \quad F_W(\sigma, \tau) = \langle f(t), \psi_{\sigma,\tau}(t) \rangle = \int_{-\infty}^{\infty} f(t) \frac{1}{\sqrt{\sigma}} \bar{\psi}\left(\frac{t-\tau}{\sigma}\right) dt \quad (2)$$

188 where $\bar{\psi}$ is the complex conjugate of ψ , and $F_W(\sigma, \tau)$ is the time-scale plot.

189 In this study, the Gaussian Derivative (GoD) was used as the mother wavelet. The
 190 real GoD wavelet component ³ in the time (t) and frequency ($s\omega$) domains can be
 191 expressed as:

$$192 \quad \psi_0(t) = \frac{(-1)^{m+1}}{\sqrt{\Gamma\left(m + \frac{1}{2}\right)}} \frac{d^m}{d\eta^m} \left(e^{-t^2/2} \right) \quad (3)$$

$$193 \quad \hat{\psi}_0(s\omega) = -\frac{i^m}{\sqrt{\Gamma\left(m + \frac{1}{2}\right)}} (s\omega)^m \left(e^{-\frac{(s\omega)^2}{2}} \right) \quad (4)$$

194 where m and Γ are wave number and Gamma function, respectively. Hence, the

195 complex wavelet form of GoD in the frequency domain can be created by using a
196 Heaviside function where the ³ wavelet decays with the square root of a gamma
197 function. In the GoD mother wavelet, the shape of the wave is essentially
198 determined by the wavelet derivative order. Thus, the best resolution of the
199 waveform can be simply obtained by varying the derivative order.

200

201 RESEARCH METHOD

202 Field Measurement

203 In the WSSW method field measurement of seismic data is done by dropping
204 steel ball bearings weighing between 5 and 15 g to generate seismic waves on the
205 pavement. Two high-frequency accelerometers (25 kHz) are employed to detect
206 the signals of seismic waves. Both accelerometer receivers are located in a linear
207 array with the source. The signals are then recorded in a set of ADT analog-digital
208 acquisition which is connected to a computer unit used to analyze the spectrum of
209 signals (Figure 1). The configuration of mid-point receiver spacings employed in
210 this study is shown in Figure 2. The field mid-point receiver spacing and receiver-
211 source spacings were arranged for sampling different depths and layers of the
212 pavement structures. The receiver spacing (as shown in Figure 2 as d_2) is less than
213 ¹⁵ and/or equal to the thickness of the layer (H). ²⁶ The distance from the source to the
214 first receiver (d_1) must be equal with the receiver spacing (d_2). Since measurement
215 was made on the surface layer of flexible and rigid pavement structures, short
216 receiver spacings of 5, 10, 15 to 30 cm were utilized. In order to enhance signal
217 quality and minimize the shifting of internal phase between receivers, the forward
218 and backward procedure of the test configuration was repeated at least 4 to 6 times
219 for each spacing measurement. This repetition was also used to verify the

220 variability and consistency of the results of the WSSW test. This paper also
221 discusses the result of the statistical analysis of the various repetition procedures.

222

223 In addition to the WSSW test, comparative tests, i.e., ² spectral analysis of surface
224 wave (SASW), falling weight deflectometer (FWD), and laboratory resilient
225 modulus tests, were also conducted at three different sites, i.e. existing flexible
226 pavement of a national road network in Purwakarta, West Java, Indonesia; a
227 campus road in Universiti Kebangsaan Malaysia (UKM), Malaysia; and a new
228 rigid pavement in Yogyakarta, Indonesia. SASW and FWD measurements were
229 made at the same locations of the road pavements. Pit test was also conducted to
230 determine the number of layer and the materials of the pavement profile. The result
231 of the pit test show that the measured pavement comprises three layers, i.e., 18 cm
232 of asphalt concrete (AC), 10 cm of crushed stone base, and 30 cm of sub-base
233 overlaying the compacted subgrade materials. Another comparative test, i.e.,
234 resilient modulus laboratory test, was conducted on existing flexible pavement at
235 the Universiti Kebangsaan Malaysia (UKM) Campus, Malaysia. The pavement
236 profile at UKM campus sites consists of an AC layer (7 cm) and a base layer of
237 crushed aggregate (40 cm) over a soil subgrade layer. The WSSW measurement
238 of rigid pavement was validated by conducting a compressive test on new PCC
239 slabs 45 cm thick over a compacted layer of sand.

240

241 **Proposed Data Analysis in the WSSW Method**

242 The following scheme for the WSSW method is proposed based on the seismic
243 data analysis using continuous wavelet transform and calculation of the elastic
244 modulus of pavement:

- 245 1. Measure the field seismic surface wave by using the mid-point receiver
 246 spacing configuration (Figure 2).
- 247 2. Compute the time-frequency spectrogram of CWT based on the Gaussian
 248 Derivative (DoG) mother wavelet for the received signal waveforms. The
 249 generated spectrogram will provide information of the varying wave modes
 250 effects, energy events of the spectrum, and the manner in which higher modes
 251 diverge in time.
- 252 3. Analyze the phase difference in the transfer function spectrum from the TF
 253 spectrograms of the signal recorded by the first and second receivers. The
 254 mathematical equation for the computation of phase spectrum is based on the
 255 wavelet spectrogram and is expressed as (Rosyidi & Taha, 2012, Rosyidi,
 256 2017):

$$257 \quad H(f) = \frac{Y(f)}{X(f)} \approx \frac{W_{f(u,s)}^Y}{W_{f(u,s)}^X} = \frac{\int_{-\infty}^{\infty} Y(t) \frac{1}{\sqrt{\sigma}} \psi^* \left(\frac{t-\tau}{\sigma} \right) dt}{\int_{-\infty}^{\infty} X(t) \frac{1}{\sqrt{\sigma}} \psi^* \left(\frac{t-\tau}{\sigma} \right) dt} \quad (5)$$

258 where,

259 $X(f)$ = signal input in the frequency domain from first receiver $X(t)$,

260 $Y(f)$ = signal output in the frequency domain from second receiver

261 $Y(t)$,

$$262 \quad W_{f(u,s)}^Y = \int_{-\infty}^{\infty} Y(t) \frac{1}{\sqrt{s}} g \left(\frac{t-u}{s} \right) e^{-i\xi(t-u)} dt \quad (6)$$

$$263 \quad W_{f(u,s)}^X = \int_{-\infty}^{\infty} X(t) \frac{1}{\sqrt{s}} g \left(\frac{t-u}{s} \right) e^{-i\xi(t-u)} dt \quad (7)$$

264 A phase spectrogram in the time-frequency domain based on Eq.6 and Eq.7

17

265 can be computed using the following equation:

$$266 \quad H(u,s) = \frac{W_f^{XY}(u,s)}{W_f^{XX}(u,s)} = \frac{|W_f^{XY}(u,s)| e^{i(\theta_Y(a,b) - \theta_X(a,b))}}{W_f^X(u,s)^* \times W_f^X(u,s)} \quad (8)$$

267 Thus, phase difference is calculated as a ratio of the imaginary to the real part
268 of the phase spectrogram, which is expressed as:

$$269 \quad \phi = \tan^{-1} \left(\frac{\Im H(u,s)}{\Re H(u,s)} \right) \quad (9)$$

270 4. Determine the coherence function spectrum to evaluate the quality of signals
271 recorded by both receivers. The coherence value is scaled in real number from
272 zero to one within the range of the measured frequencies. A value of one
273 indicates a good signal and the best correlation between the two observed
274 signals while a value of zero indicates a bad signal and lack of correlation
275 between the two signals. The coherence function was obtained by using the
276 following formula (Rosyidi, 2017):

$$277 \quad \gamma^2(f) = \frac{W_f^{yx}(u,s) \cdot W_f^{yx}(u,s)^*}{W_f^{xx}(u,s) \cdot W_f^{yy}(u,s)} \quad (10)$$

278 5. Generate a trendline of linear regression relationship from phase difference
279 versus frequency. 30 Phase velocity is then calculated as a function of the slope
280 value (m) of linear regression line. The mathematical formulation for the phase
281 velocity and the slope is expressed as:

$$282 \quad \phi = \left| \frac{360D}{V_{ph}} \right| f = mf \quad (11)$$

283 The phase velocity given by Equation 11 is 2 determined from the slope of the
284 obtained best-fit line (m). In this formulation, the phase velocity is assumed to
285 be independent of the wavelength with a value approximately equal to the

286 thickness of the uppermost layer. The range of the wavelength can be
287 assessed from the relationship of phase velocity and its frequency (f):

$$288 \quad \lambda = \frac{V_{ph}}{f} \quad (12)$$

289 6. Calculate the dynamic elastic modulus (E) of the pavement materials by using
290 Formulas 13 and 14 (Baker et al, 1995):

$$291 \quad E = \frac{Y}{g} |KV_{ph}|^2 \quad (13)$$

$$292 \quad K = (1.13 - 0.16\mu) \sqrt{\frac{2(1-\mu)}{1-2\mu}} \quad (14)$$

293 where V_{ph} is phase velocity, g is acceleration of gravity, γ is total unit weight
294 of the material, and μ is the assumed Poisson's ratio. It should be noted that, in
295 the WSSW technique, the materials on surface layer of the pavement are
296 assumed to be uniform when the
297 high-frequency surface waves were generated.

298

299 **RESULTS AND DISCUSSION**

300 **Application of WSSW on Flexible Pavement**

301 **In situ Measurement of the Elastic Modulus of Surface Layer**

302 WSSW tests were carried out at twelve locations of road-flexible pavements on
303 the national highway network in Purwakarta, Indonesia. Figure 3 shows the
304 example of the signals from the WSSW measurement. The groups of body and
305 surface waves from the recorded signals can be explored, as shown in Figure
306 3. These signals were used to generate a time-frequency (TF) spectrogram plot by
307 using the CWT of GoD. The spectrogram of CWT can be used to solve the
308 problems of identifying spectral events of the seismic signals obtained from field

309 measurement. The spectrogram shows the energy of measured signals as a linear
310 combination in signal which is shifted by Gaussian Derivation functions in time
311 and frequency domain. This technique is effectively used for a good tool in
312 investigation of wave group in energy events. A typical CWT spectrogram in the
313 time-frequency resolution plot of the signals is shown in Figure 4. It shows two
314 distinct energy from the wave propagation events in the wavelet spectrogram. The
315 energy amplitude distribution in both spectrograms are displayed in a normalized-
316 dB unit. The wave group which arrived early has been identified as a lower mode
317 of seismic waves. The frequency band of the lower energy ranges from 2.8 to 16
318 kHz. Within this spectrum range, the wave mode has been identified as coming
319 from the surface wave signals. The energy level of the lower mode of seismic
320 signals can detect up to 60 % of total wave energy through independent
321 measurement of surface wave propagation. The wave group which arrived later
322 was identified from direct and reflected body waves. The waves which arrived later
323 have higher frequency and is the higher mode of seismic waves. This mode
324 occurs at frequencies greater than 16 kHz. The result of the CWT spectrogram
325 indicates that the dominant wave energy of the surface waves at the frequency
326 range of interest can be clearly observed. The spectrogram provides information on
327 wave mode with a clear time-frequency resolution at high frequency signals. It can
328 be used to interpret the group frequency bandwidth by using various derivation
329 order of the Gaussian mother wavelet.

330

331 Figure 4 shows the calculated phase difference of seismic signals in the frequency
332 domain which were determined from both wavelet spectrograms. Without
333 information on the observed energy wave groups, the wrapped phase could

334 produce erroneous phase velocity. The separation of energy wave group of interest
335 can be done by extracting the selected dominant energy event of surface wave
336 group from the CWT spectrogram. In this study, the energy event of surface wave
337 detected between 2.8 to 16 kHz was extracted and the wrapped phase difference
338 was then measured from the transfer function spectrum, as shown in Figure 5. The
339 wrapped phase data is represented with a value of between $-\pi$ and π radian (or -180
340 and 180 degrees) which makes it easier to observe the detailed variation in the
341 phase data in a small space of graph. By using the wavelet spectrogram approach
342 to extract the selected energy wave group of surface waves, the phase difference
343 from transfer function spectrum shows clear saw-tooth patterns since the phase
344 spectrum for the most part carries the dominant energy event of a wave group at a
345 given frequency. It also shows that the time-frequency CWT spectrogram of the
346 Gaussian Derivative wavelet can be effectively used to generate enhanced phase
347 spectrum with a better, smooth, clear pattern than the traditional phase unwrapping
348 by Fourier analysis that is usually done in the SASW. Figure 6 compares the phase
349 spectrum obtained by using CWT and Fourier analysis. The transient wave pattern
350 from seismic waves is usually sparse in the wavelet (Ching et al., 2004). Their
351 investigation shows that, compared to the Fourier domain, the wavelet domain is a
352 better platform for estimating the function for transient wave pattern since the
353 pattern can be easily differentiated from the signals, higher mode reflected signals,
354 and noise. Another related work by Gucunski and Shokouhi (2005) proved the
355 advantage of using wavelet transform in spectral analysis since it is capable of
356 giving a more stable computation of phase velocity and can be used to characterize
357 layer interface. In this study, WSSW can be used to characterize and extract the
358 energy event of wave groups from the surface wave and reflected body waves.

359 Figure 6 shows a comparison of the wrapped phase spectrum generated through
360 Fourier analysis and wavelet analysis. It is interesting to note that the wavelet
361 analysis extracted from phase spectrum of interest produced a better and smoother
362 pattern compared to the Fourier domain, as discussed above.

363

364 Figure 5 shows that the phase difference spectrum has a clear saw-tooth pattern in
365 the frequency domain of up to 25 kHz. With regards to the phase data, the high-
366 frequency mode of surface waves is represented as a pavement surface layer with a
367 high stiffness (elastic modulus). In this case, the coherence function was used to
368 inspect the quality of phase difference spectrum. Figure 6 shows that the phase
369 data with a frequency of up to 20 kHz has a coherence magnitude greater than
370 0.98.

371

372 For a given phase difference spectrum, the elastic modulus of a pavement surface
373 layer can be calculated by fitting a smooth curve of the weighing function. The
374 smoothed phase spectrum was generated and fitted to the raw data points of phase
375 difference. The phase spectrum was then unwrapped by counting the number of
376 cycles from the peak sequence of the wrapped phase spectrum, as shown in Figure
377 7. The linear regression analysis was then generated on the phase spectrum as the
378 best fit trendline of the phase difference. The slope of the line is almost similar
379 with the measured frequency. The value of the slope was then substituted into
380 Equations 11, 13 and 14 to determine the elastic modulus of the surface layer
381 material. As can be seen in Figure 7, the trendline for the frequency range
382 coincides with the wavelengths that are less than the thickness of the surface layer.

383

384 Figure 7 shows that the slope (m) of the trendline has a value of 0.0140 and is the
385 best-fit curve. Using Equation 13 to compute the phase velocity gives a value of
386 1,028.57 m/s. By using the calculated phase velocity, a field configuration with a
387 receiver spacing (d_2) of 5 cm; assumed Poisson's ratio of 0.25 for pavement
388 material such as asphaltic (Asphalt Concrete/AC) layer; and a unit weight of 2,200
389 kg/m^3 , the elastic modulus was then computed to be 845,662,040.80 kg/m^2
390 (8,456.62 MPa). This value was obtained when measurement was made at a
391 pavement surface temperature of 31.8°C. The measured modulus is the typical
392 value of an AC modulus when measured at a small strain level, which is similar to
393 the findings made by Nazarian and Stokoe (1986), Stokoe et al. (1991), Roesset et
394 al. (1991), Aouad et al. (1993), Aouad et al. (2000), and Yuan et al. (2015). Aouad
395 et al. (1993) have proven that the seismic method is effective for determining in
396 situ changes in stiffness (E) at temperatures ranging from 30°F to 143°F.

397
398 In general, this result indicates that the elastic modulus of the pavement surface
399 layer can be simply determined by using the WSSW technique. However, the
400 elastic modulus obtained in this study are relatively high. This is because the
401 seismic technique evaluates the modulus at a very low strain level (less than 10³
402 %). The behavior of material modulus at this strain level could be considered as
403 the maximum moduli due to its very small strain amplitude. This finding is
404 supported by a previous observation made by Roesset et al. (1990). In addition, if
405 the elastic modulus of asphalt concrete is a function of frequency, the modulus
406 obtained from seismic measurement will give higher stiffness values than other
407 dynamic and static tests due to the high frequency used in the seismic tests.
408 Consequently, adjustment should be made to the seismically determined stiffness

409 (Stokoe et al. 1991) by constructing a master curve for temperature correction and
410 frequency shift (Kweon and Kim, 2006; Ryden, 2011; Gudmarsson et al. 2012). In
411 the attempt to illustrate the sensitivity and utility of WSSW method for measuring
412 changes in stiffness, in situ WSSW tests were performed on constructed road-
413 pavement and pavement overlay. Figure 8 shows that the different layers of
414 stiffness of both pavement profile have been investigated satisfactorily. The road-
415 pavement surface and overlay layer were evaluated using a 10- and 5-cm receiver
416 spacing configuration, respectively. The properties of both surface layers were
417 determined definitively without any complex inversion process that is usually
418 required in the SASW method. The change in the stiffness of the surface layer can
419 also be evaluated non-destructively and quickly by using the WSSW technique.
420 The WSSW method, however, can only be used in two obvious conditions: first, it
421 is only effective when the wavelength is less than and/or equal to the uppermost
422 thickness of surface layer. When the wavelength is greater than thickness of the
423 layer, the dispersive surface wave velocity is significant influenced. Secondly, the
424 material properties of the pavement surface layer are assumed to be uniform and
425 modulus is measured at very low strain levels and high levels of frequency. The
426 elastic theory is used to explain the response of material associated with this
427 measurement where the response of material is predominantly linear (Luna & Jadi,
428 2000).

429

430 **Validation by using the SASW and FWD Test**

431 As shown in Figure 8, the result was then validated by conducting spectral-
432 analysis-of-surface-wave (SASW) tests at the same locations where the WSSW
433 tests were performed. In the SASW method, impact sources, i.e. ball bearings and

434 hammers, were used to produce the energy of surface wave propagating
435 horizontally in the sub-surface layer of the pavement. Various receiver and source
436 configurations were used with mid-point receiver spacings of 5, 10, 20, 40, 80 and
437 160 cm to examine the pavement profile. Short receiver spacings of 5 and 10 cm
438 were used with ball bearings as a source of high frequency to sample the pavement
439 surface layers; longer receiver spacings of 20 to 160 cm were used along with
440 small- to medium-sized sledge hammers as low frequencies sources to observe the
441 response of base and subgrade layers. DJB A/123/E piezoelectric accelerometer
442 and Harmonic 01 dB (IEC 651-804 Type-I) ADC (analog digital converter) were
443 connected to a computer and were used to receive and record both high and low
444 frequency seismic waves. Fast Fourier Transform was used to compute the phase
445 difference based on the signals and was displayed in the cross-power spectrum.
446 The phase information was then unwrapped and analyzed to produce a dispersion
447 curve of phase velocity versus wavelength. Figure 9 shows an example of the
448 composite experimental dispersion curve from the measurements made by all
449 receiver spacings. Subsequent to obtaining the dispersion, inversion analysis was
450 done based on the established theoretical model. In this analysis, the 3-D stiffness
451 matrix model proposed by Kausel and Peek (1982) was used. The final profile of
452 shear wave velocity was obtained after 16 iterations with a root-mean-square error
453 (RMS) of 35.47 m/s or an average deviation of about 5.92 %.

454

455 Figure 10 shows the equivalent shear wave profile obtained after inversion while
456 Figure 11 shows the equivalent dynamic elastic modulus profile which was
457 obtained using the dynamic material equation. The modulus profile in Figure 11 is
458 only valid at a depth of 10 cm where the asphaltic layer is located. The elastic

459 modulus shown in the figure is congruent with the elastic modulus obtained when
460 using the WSSW and SASW methods. The difference between the two methods
461 is 0.01 % and 1.14 % for the first and second layer of pavement surface,
462 respectively.

463

464 The ⁴ falling weight deflectometer (FWD) method was used to verify the elastic
465 modulus of pavement surface layer obtained through the WSSW test. Figure 12
466 shows the ⁵ elastic modulus of pavement surface layer obtained using both the FWD
467 and WSSW methods. The elastic modulus obtained using WSSW is higher than
468 the value obtained through the ⁵ FWD test. As mentioned previously, the modulus
469 measured at very low strain levels in the surface wave method is the maximum
470 value, has a high loading frequency, and is not determined by strain amplitude.
471 Contrarily, in the FWD test, the modulus was obtained from backcalculation of in
472 situ measurement of deflection basins. In this test, a falling weight was dropped to
473 obtain a target load of 40 kN in order to generate pavement basins. Nazarian et al.
474 (1999) and Stokoe et al. (1991) reported that the modulus measured in a FWD test
475 usually corresponds with the secant modulus of the ² materials close to the loading
476 pad (i.e. pavement surface layer and base/subbase layer) and the ² initial tangent
477 modulus for the materials further from the impact/dropped weight (deeper
478 subgrade). On the contrary, the modulus obtained by using the proposed WSSW
479 method is measured directly ² using a small seismic source. The modulus thus
480 obtained always corresponds with the initial tangent modulus due to the small
481 impact. This is the reason why the modulus obtained from the proposed WSSW is
482 higher than that obtained via the FWD method. However, as presented in Figure
483 13, a correlation of data trend from field testing shows that the lower modulus

484 obtained through the FWD method is also measured at lower modulus level when
485 using the WSSW. Additionally, the high frequency of the seismic method
486 generated greater stiffness values for pavement material. Roesset et al. (1990)
487 found that frequency has a significant effect on modulus value at the small strain
488 levels in the seismic and FWD tests. In FWD, modulus was measured at a
489 frequency of approximately 30 Hz (Figure14) calculated from peak frequency of
490 displacement in the auto-spectrum of wave propagation energy recorded by the
491 geophones. This is congruous with the results obtained by Stokoe et al. (1991).
492 These researchers measured the auto-spectrum of the velocity resulting from the
493 impact of an FWD on AC pavement layer. The results of their study show that the
494 impact energy of FWD is concentrated in a frequency range of 2 to 50 Hz with a
495 peak energy of between 25 to 30 Hz. The peak frequency response of FWD
496 obtained in the present study is similar with that obtained by Roesset et al. (1990)
497 where the frequency of FWD was found to be 30 Hz.

498

499 **Validation with Resilient Modulus Test**

500 In this section, the results obtained via the WSSW test is compared with the result
501 of laboratory resilient modulus (M_r) test conducted at same location of the road
502 pavement on the UKM Campus, Bandar Baru Bangi, Malaysia. WSSW test with
503 identical configuration was conducted at 30 observation points and the data was
504 then processed as described in the previous section. After completing the WSSW
505 test, the specimens of the pavement surface layer to be used for laboratory resilient
506 modulus were cored from the same location. Laboratory resilient modulus, M_r , is
507 the elastic modulus based on recoverable strain under repeated load. The test was
508 conducted in accordance with the ASTM D 4123 under indirect tensile mode using

509 a Universal Testing Machine (UTM). In the resilient modulus test, the time
510 dependent deformation by using constant compressive stress was set up to assess
511 the ability of the cored specimen to recover from repeated loading without
512 reaching failure limit. In this test, the specimens were tested in two orientations,
513 i.e. 0° and 90°. The resilient modulus was computed by assuming a Poisson's ratio
514 of 0.35. A typical result for the resilient modulus obtained from a laboratory test
515 of the sample cored from the road pavement on the UKM campus is presented in
516 Table 1. The AC core was tested at a temperature of 36°C. This temperature is
517 similar with the field temperature when the WSSW test was conducted. Table 1
518 presents the results for air voids, tensile strain, indirect tensile strength, and
519 resilient modulus test obtained from the measurement of the cored samples of the
520 two testing sites. Statistical analysis of coefficient of variation (CV) and range of
521 acceptance (RA) indicate that the results of resilient stiffness data are statistically
522 sound.

523

524 The resilient modulus of all specimens and WSSW tests are presented in Figures
525 15 and 16. Figure 15 presents the regression analysis of elastic modulus for the
526 resilient modulus test and WSSW test at a surface layer temperature of 36°C. The
527 moduli obtained from the WSSW and laboratory resilient modulus tests are plotted
528 on the y -axis and the strain levels obtained from each measurement of the
529 specimens are plotted on the x -axis (Figure 16). Similar with the results of the
530 FWD test, the value of elastic modulus obtained from the WSSW test is higher
531 than the value produced by the laboratory resilient modulus test. This difference
532 is due to the different strain levels in both tests. The elastic modulus from the
533 WSSW test is a maximum value and is independent of strain amplitude.

534

535 **Application of WSSW on Rigid Pavement**

536 **In situ Measurement of Elastic Modulus**

537 WSSW measurements were also made on a new rigid pavement in Yogyakarta,
538 Indonesia. The tests were conducted on slabs fabricated using ⁶concrete class Type
539 I cement with a maximum aggregate size of 0.019 m. The concrete mixtures for
540 ⁶the PCC slab casts were designed to have a minimum 28-day compressive strength
541 of 225 kg/cm² (22.04 MPa). The concrete has a ⁶cement-water ratio of 0.48 and an
542 average slump of 0.033 m. The 450-mm thick PCC slabs were placed over a
543 compacted layer of sand on subgrade soil. The tests were conducted on the slabs
544 after a curing time of 3, 14, and 28 days.

545

546 Figure 17 shows a typical result of time frequency spectrogram of GoD CWT
547 from the measured signals. Signals were recorded with a field measurement
548 configuration of 30 cm receiver spacing (D) on a PCC slab with a 14-day curing
549 time. Figure 17 clearly shows that several signal energy groups ³at different
550 frequency bands were detected, which could result in interference at low and
551 higher mode of signals. The wave energy events occurred within 0.02 to 0.026
552 seconds of arrival time (received by accelerometers). It shows that the dominant
553 energy event occurred between 5 to 25 kHz in both signal CWT spectrograms.
554 Within this range, the events were investigated as energy group of surface waves
555 and interference of reflected body waves. The first energy group occurred at a high
556 frequency of between 5 to 16 kHz (channel 1) and 6 to 16 kHz (channel 2), which
557 are identified as surface wave propagation.

558

559 The unwrapped raw phase spectrum was then computed and is shown in Figure 18.
560 A linear regression ($y = mx$) of phase angle versus frequency was generated, and
561 the best-fit line has a slope (m) of 0.0535. The phase velocity was calculated based
562 on the slope value and receiver distance using Equation 11 and was found to be
563 2,018.69 m/s. The unit weight of concrete in the PCC slabs were measured at each
564 elapsed time of the curing process. By assuming a Poisson's ratio and unit weight
565 of concrete material for a 3-day curing time of 0.20 and 2,420 kg/m³, respectively,
566 the elastic modulus of rigid pavement surface layer were obtained using Equations
567 13 and 14 and was found to be 23,660.99 MPa (23.66 GPa). Figure 19 shows the
568 measured elastic modulus for concrete PCC slabs at 3-, 14- and 28-day curing
569 time. It shows that WSSW test can also be used to monitor any changes in the
570 stiffness of the surface layer of rigid pavement during the curing of PCC slabs.

571

572 **Validation with Laboratory Compressive Strength Test**

573 A laboratory compressive test was conducted to validate the value of the stiffness
574 of rigid pavement obtained via the WSSW tests; the test was performed using a
575 standard 6 by 12-in cylinder sample in accordance with compression tests standard
576 ASTM C 39. The compressive tests were conducted to determine the average
577 compressive strength of three cylinders of PCC slab samples. The compression
578 tests were conducted 3, 14 and 28 days after casting. The results for the
579 compressive strengths are presented in Table 2. Figure 12 shows that elastic
580 modulus obtained via the WSSW tests is in good agreement with the compressive
581 strength obtained via the laboratory test with a coefficient of determination of
582 0.995. This indicates the feasibility of using WSSW to make a quick measurement
583 and predict the elastic modulus of the surface layer (PCC Slab) of rigid pavements.

584

585 **CONCLUSION**

586 This paper introduces a technique for determining the surface layer stiffness of
587 flexible and rigid pavements by performing a ⁹ wavelet-spectrogram analysis of
588 surface waves (WSSW). The technique employs a ³ time-frequency analysis of
589 continuous wavelet transforms (CWT) spectrogram to identify energy events, filter
590 the wave modes of interest, and improve the quality of phase spectrogram of the
591 received seismic signals. The technique is also capable of enhancing the transfer
592 function spectrogram used to obtain the phase difference data. By using a simple
593 formulation of phase spectrum slope and material properties of the pavement, the
594 ¹² elastic modulus of a pavement surface layer can be determined without having to
595 perform any complex inversion analysis. The WSSW method is a non-destructive
596 test which can be used for regular monitoring of the changes in the elastic
597 modulus of constructed pavement surface and its overlays.

598

599 **ACKNOWLEDGMENTS**

600 This work is a part of a research project funded by the Ministry of Research,
601 Technology and Higher Education, Indonesia under the research scheme of PUPT
602 (Penelitian Unggulan Perguruan Tinggi) No. SP DIPA-023.04.1.673453/2015;
603 Universitas Muhammadiyah Yogyakarta (UMY), and Universiti Kebangsaan
604 Malaysia (UKM) project number UKM (DIP-2017-004). Their supports are
605 gratefully acknowledged. We would like to thank Dr. Siegfried (Puslitbang Jalan,
606 Bandung) and the research assistants for their cooperation during field work.

607

608 **REFERENCES**

- 609 Al-Hunaidi, M. O. (1992). Difficulties with phase spectrum unwrapping in spectral
610 analysis of surface waves nondestructive testing of pavements. Canadian
611 Geotechnical Journal. doi: 10.1139/t92-055
- 612 Aouad, M., Stokoe, K.H., II and Briggs, R.C. (1993). Stiffness of Asphalt Concrete
613 Surface Layer from Stress Wave Measurements. Transportation Research
614 Record 1384, 29-35.
- 615 Aouad, M., Stokoe, K.H., II and Joh, S-H. (2000). Estimating Subgrade Stiffness
616 and Bedrock Depth: Combined Falling Weight Deflectometer and Simplified
617 Spectral Analysis of Surface Waves Measurements. Journal of the
618 Transportation Research Board, Transportation Research Record. doi:
619 10.3141/1716-05
- 620 Baker, M.R., Crain, K. and Nazarian, S. (1995). Determination of pavement
621 thickness with a new ultrasonic device. Research project 7-1966, The Center for
622 Geotechnical and Highway Materials Research, The University of Texas at El
623 Paso.
- 624 Ching, J., To, A.C. and Glaser, S.D. (2004). Microseismic source deconvolution:
625 Wiener filter versus maximax, Fourier versus wavelets and linear versus
626 nonlinear. J. Acoustical Society of America, 115 (6). doi: 10.1121/1.1705658
- 627 Foughoula-Georgiou, E. and Kumar P. (1995). Wavelets in Geophysics. Academic
628 Press.

629 Ganji, V. *et. al.* (1998). Automated inversion procedure for spectral analysis of
630 surface waves. *Journal of Geotechnical and Geoenvironmental Engineering*,
631 ASCE. doi: 10.1061/(ASCE)1090-0241(1998)124:8(757)

632 Gucunski, N. and Shokouhi, P. (2005). Wavelet transforms in surface wave
633 analysis. *Geotechnical Special Publication 134 Soil Dynamics Symposium in*
634 *Honor of Professor Richards D. Woods*, ASCE.

635 Gudmarsson, A., Ryden, N., and Birgisson, B. (2012). Characterizing the low
636 strain complex modulus of asphalt concrete specimens through optimization of
637 frequency response functions. *Journal of Acoustical Society of America*. doi:
638 doi: 10.1121/1.4747016

639 Hazra Sutapa and Kumar Jyant (2014). SASW testing of asphaltic pavement by
640 dropping steel balls. *International Journal of Geotechnical Engineering*, Taylor
641 & Francis. doi. 10.1179/1938636213Z.00000000051

642 Heisey, J. S., Stokoe, K. H., and Meyer, A. H. (1982). Moduli of pavement
643 systems from spectral analysis of surface waves. *Transportation Research*
644 *Record 852*, Transportation Research Board.

645 Kausel E. and Peek R. (1982). Dynamic loads in the interior of layered stratum: An
646 explicit solution. *Bulletin of Seismology Soc. Am* 72:5, 1459–1481.

647 Kim D.S. *et. al.* (2001). Evaluation of density in layer compaction using SASW
648 method. *Soil Dynamic and Earthquake Engineering*, Elsevier.
649 doi:10.1016/S0267-7261(00)00076-2

650 Kweon, G. and Kim, Y. (2000). Determination of asphalt concrete complex
651 modulus with impact resonance test. *Journal of the Transportation Research*
652 *Board*, *Transportation Research Record*. doi: 10.3141/1970-18

653 Luna, R. and Jadi, H. (2000). Determination of dynamic soil properties using
654 geophysical methods. *Proceedings of the First International Conference on the*
655 *Application of Geophysical and NDT Methodologies to Transportation*
656 *Facilities and Infrastructure*, St. Louis, MO.

657 Nazarian, A. and Stokoe, K.H., II. (1986). In situ determination of elastic moduli
658 of pavement systems by spectral-analysis-of-surface-waves method (theoretical
659 aspects). *Research report No. 437-2*, Center for Transportation Research, The
660 University of Texas at Austin.

661 Nazarian, S., Yuan, D. and Tando, V. (1999). Structural Field Testing of Flexible
662 Pavement Layers with Seismic Methods for Quality Control. *Journal of the*

663 Transportation Research Board, Transportation Research Record. doi:
664 10.3141/1654-06

665 Roesset, J.M., Chang, D-W., Stokoe, K.H., II and Aouad, M. (1990). Modulus and
666 thickness of the pavement surface layer from SASW test. Transportation
667 Research Record, Vol. 1260, Transportation Research Board.

668 Rosyidi S.A.P. (2017). Wavelet-Spectrogram Analysis of Surface Wave Technique
669 for Quick NDT Measurement on Surface Layer of Pavement. In: Mohammad L.
670 (eds) Advancement in the Design and Performance of Sustainable Asphalt
671 Pavements. GeoMEast 2017. Sustainable Civil Infrastructures. Springer, Cham.
672 doi:10.1007/978-3-319-61908-8_19

673 Rosyidi S.A.P. *et. al.* (2009). Signal reconstruction of surface waves on SASW
674 measurement using Gaussian derivative wavelet transform. Acta Geophysica,
675 Springer. doi: 10.2478/s11600-009-0015-8

676 Rosyidi S.A.P. (2015). Simultaneous in-situ stiffness and anomalies measurement
677 on pavement subgrade using tomography surface waves technique. Procedia
678 Engineering, Elsevier. doi:10.1016/j.proeng.2015.11.057

679 Rosyidi S.A.P. and Taha M.R. (2012). Wavelet spectrogram analysis of surface
680 wave technique for dynamic soil properties measurement on soft marine clay
681 site. Seismic Waves - Research and Analysis, Intech. doi: 10.5772/27530

682 Rosyidi S.A.P. *et. al.* (2007). Development of VS-CBR-DCP empirical model for
683 determining dynamic stiffness of pavement base layer using SASW.
684 Proceedings of International Conference on Advanced Characterisation of
685 Pavement and Soil Engineering Materials, pp.895-902.

686 Ryden, N. *et. al.* (2004). Multimodal Approach to Seismic Pavement Testing.
687 Journal of Geotechnical and Geoenvironmental Engineering, ASCE. doi:
688 10.1061/(ASCE)1090-0241(2004)130:6(636)

689 Ryden, N. (2011). Resonant frequency testing of cylindrical asphalt samples.
690 European Journal of Environmental and Civil Engineering, doi:
691 10.1080/19648189.2011.9693349

692 Stokoe, K.H., II, Hudson, W.R. and Miner, B.F. (1991). The falling weight
693 deflectometer and the spectral analysis of surface wave test for characterizing
694 pavement moduli: a case study. Research Report No. 1123-7F, Center for
695 Transportation Research, The University of Texas at Austin. Stokoe II K.H. *et.*
696 *al.* (1994). Characterization of geotechnical sites by SASW method.

697 Geotechnical characterization of sites. R.D. Wood, Ed., Oxford and IBH
698 Publishing Co., New Delhi, India, pp.15-26.

699 Tokimatsu, K. *et. al.* (1992). Effects of multiple modes on Rayleigh wave
700 dispersion characteristics. Journal of Geotechnical Engineering, ASCE.
701 doi:10.1061/(ASCE)0733-9410(1992)118:10(1529)

702 Yuan, J., Zhu, J. and Kim, C. (2015). Comparison of SASW and MASW methods
703 using MSOR approach – a case study. International Journal of Geotechnical
704 Engineering. doi: 10.1179/1938636213Z.00000000077

705 Yusoff N.I.M *et. al.* (2015). Measurements of the elastic modulus of pavement
706 subgrade layers using the SASW and FWD test methods. The baltic journal of
707 road and bridge engineering, Vilnius: Technika. doi: 10.3846/bjrbe.2015.22

708

709

710

711

712

713

714

715

716

717

718

719

720

721

722

723

724

725 **TABLE**

726 Table 1. Typical result of indirect tensile and resilient modulus tests conducted on
 727 the sample of AC cored from a pavement-road on the UKM Campus, Malaysia

Sta	Sampel No.	Air Voids (%)	$\mu\epsilon$ (tensile)	σ (tensile)	M _R (MPa)
0+200	A-1	5.06	118.90	211.90	1735
0+200	A-2	5.32	120.10	214.60	1739
0+200	A-3	4.89	148.10	261.70	1720
	Mean	5.09	129.03	229.40	1731
	SD*				10.02
	CV*				0.58%
	RA*				1.64%

Sta	Sampel No.	Air Voids (%)	$\mu\epsilon$ (tensile)	σ (tensile)	M _R (MPa)
0+300	B-1	4.65	84.44	2070	2388
0+300	B-2	5.12	85.03	204.50	2343
0+300	B-3	4.64	85.63	203.30	2312
	Mean	4.80	85.03	204.90	2347
	SD*				38.21
	CV*				1.63%
	RA*				4.61%

728

729

730

731

732

733

734

735

736

737

738

739

740

741

742 Table 2. Average compressive strength of PCC slabs of a new rigid pavement after

743 varying curing time

Elapsed time (curing period) in days	No. PCC Slabs Sample Test	Average Elastic Modulus from WSSW Test (MPa)	Average compressive strength of PCC Slab (MPa)
3	1	23,660	14.2
	2	22,980	14.6
	3	23,420	13.9
14	1	31,130	25.0
	2	30,760	24.3
	3	31,250	24.9
28	1	33,560	28.3
	2	34,070	28.9
	3	33,810	27.9

744

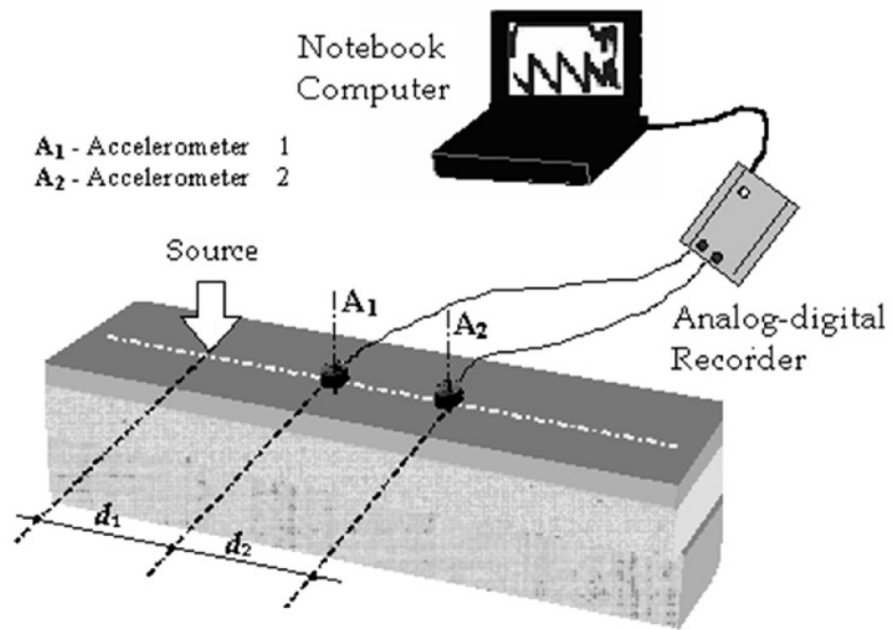


Figure 1. Experimental set up for WSSW measurement on a pavement structure

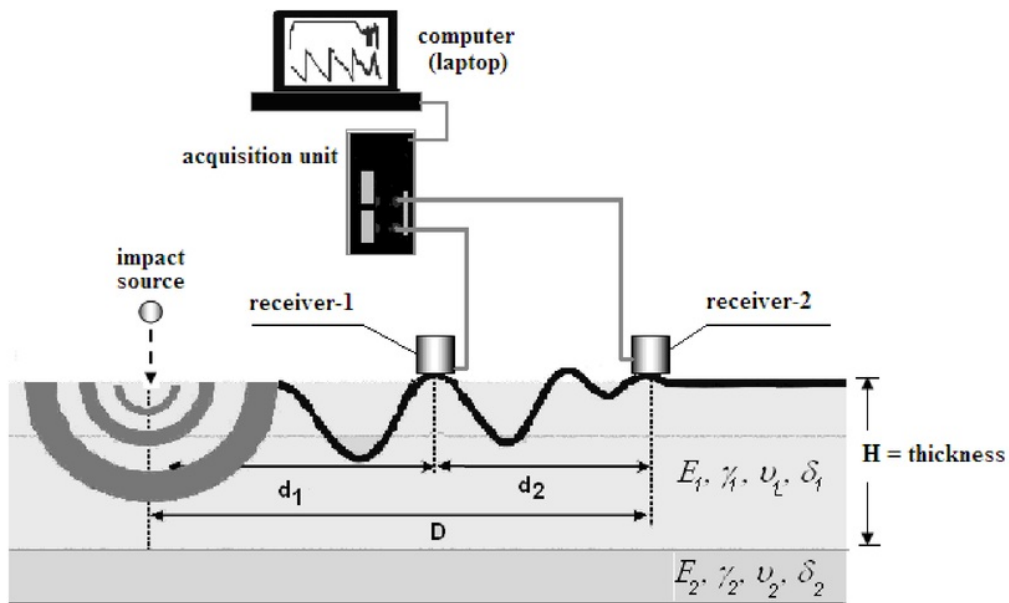


Figure 2. Mid-point receiver configuration for WSSW measurement on pavement structure

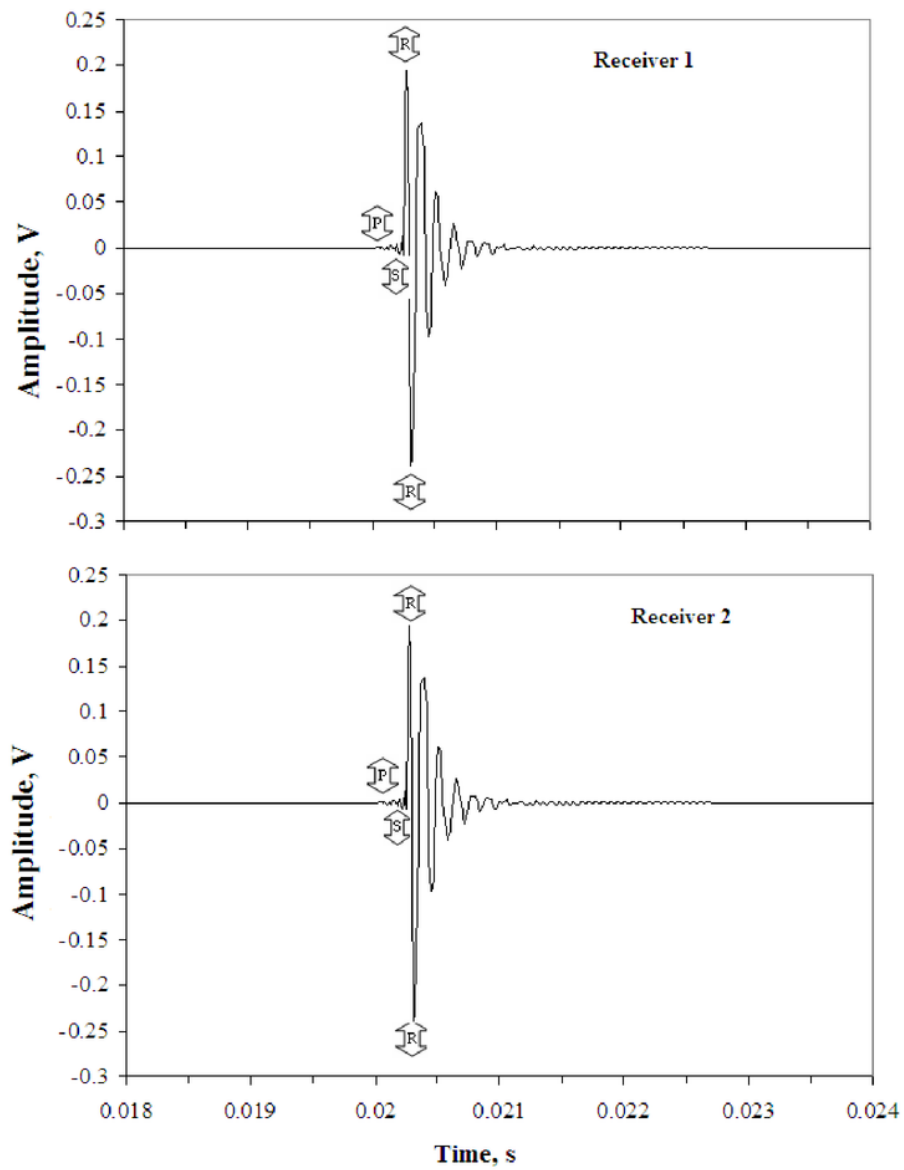
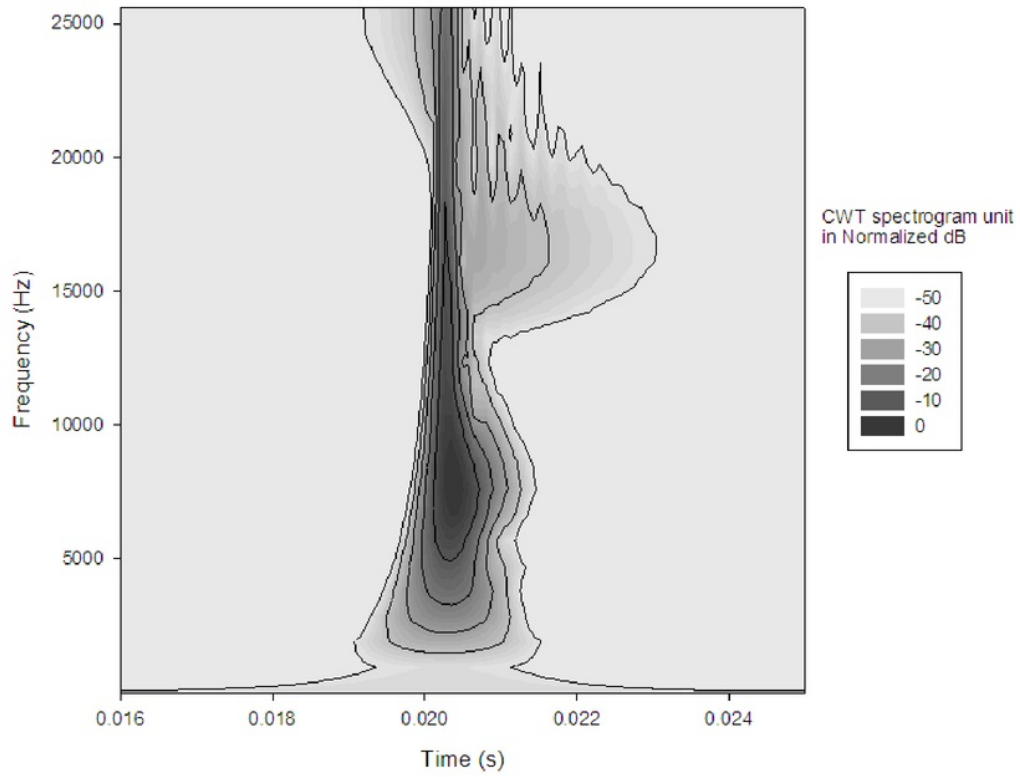
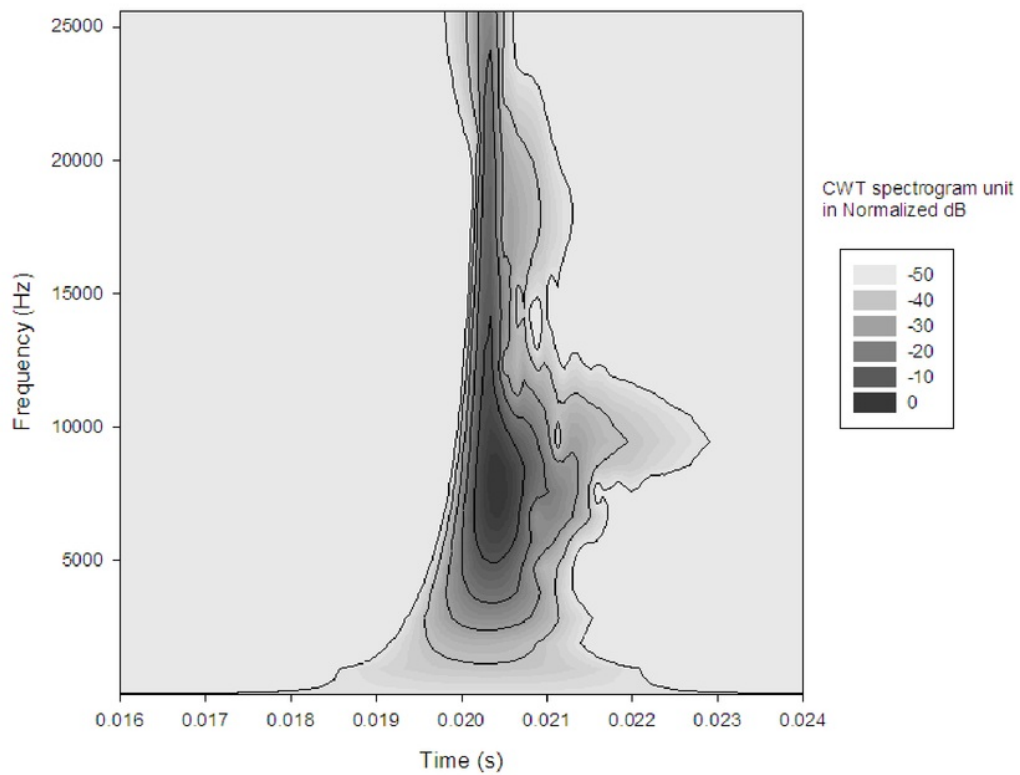


Figure 3. Typical signals from WSSW measurement on a pavement structure



(a) CWT Spectrogram displayed in normalized-dB energy amplitude distribution from receiver 1



(b) CWT Spectrogram displayed in normalized-dB energy amplitude distribution from receiver 2

Figure 4. Time-frequency plot of received signals from WSSW measurement at national road pavement site in Purwakarta, Indonesia

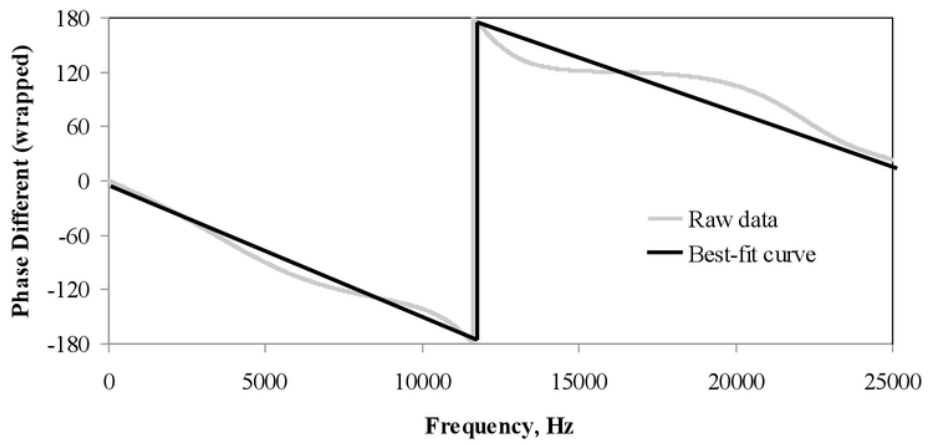


Figure 5. Comparison of raw data and best-fit curve of wrapped transfer function spectrum based on measurements

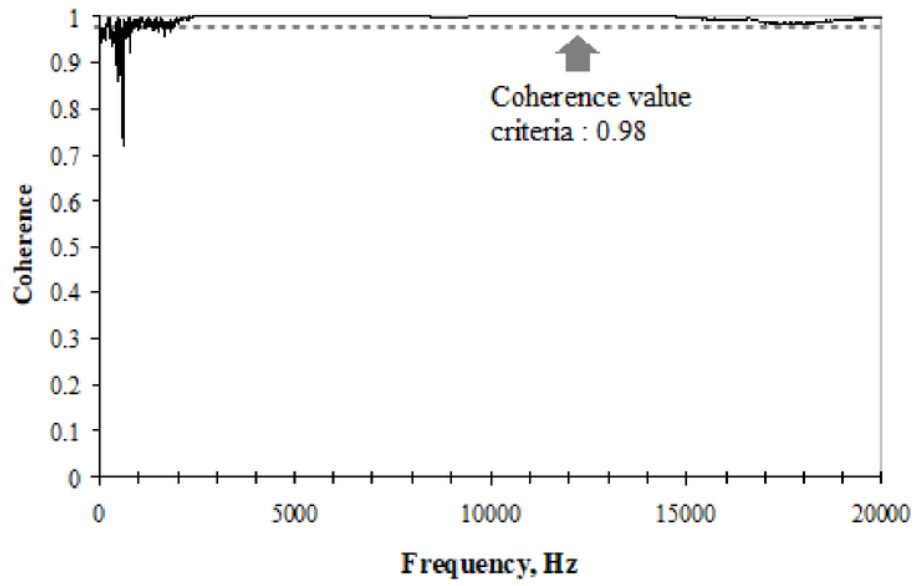


Figure 6. Coherent function spectrum of received signals from measurement

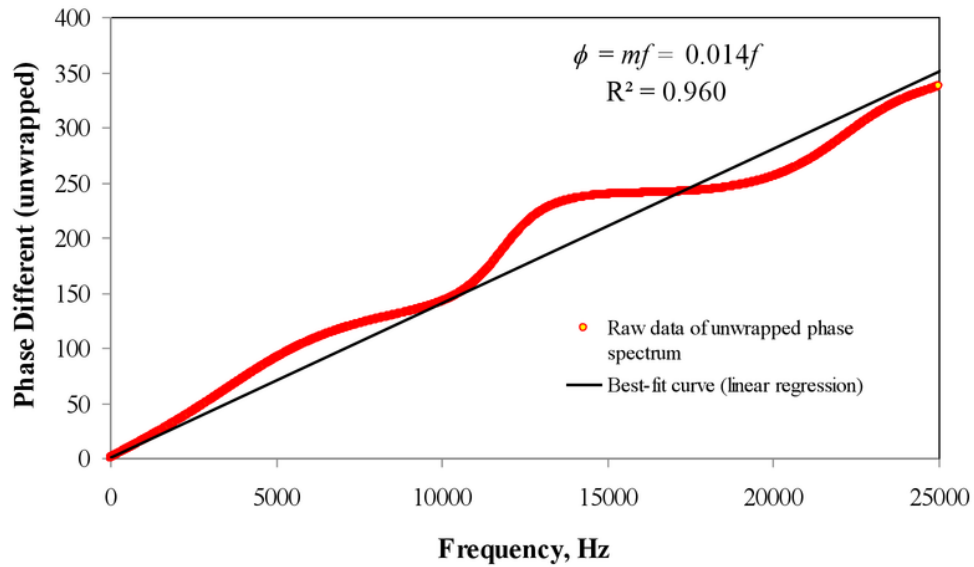


Figure 7. Linear relationship of phase difference and frequency in the unwrapped transfer function for obtaining the slope (m) parameter at flexible pavement site in Purwakarta, Indonesia

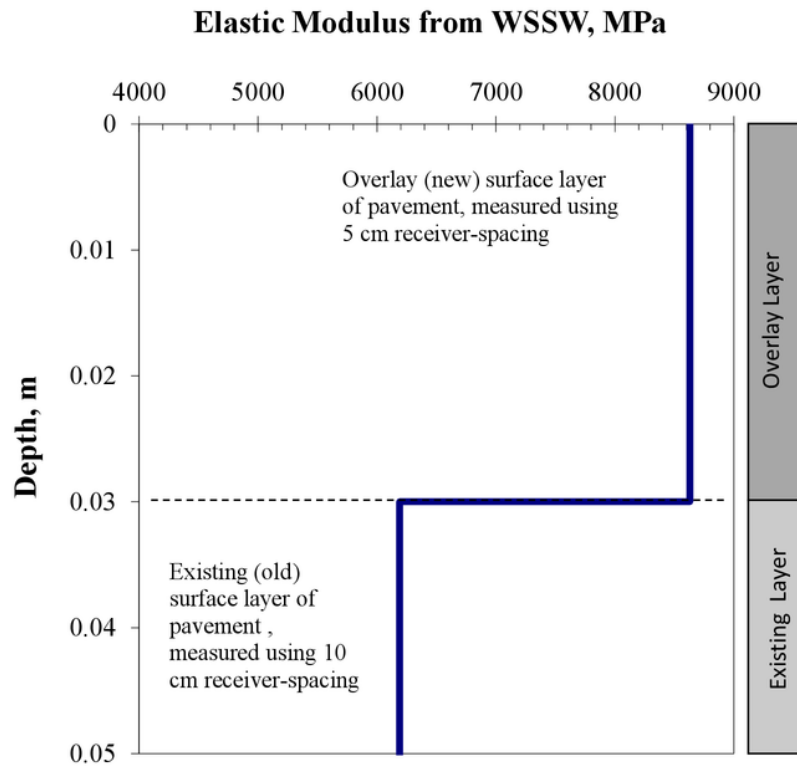


Figure 8. Elastic modulus profile of pavement obtained using the WSSW method for an overlay and existing surface layer of a flexible pavement test site at Purwakarta, Indonesia

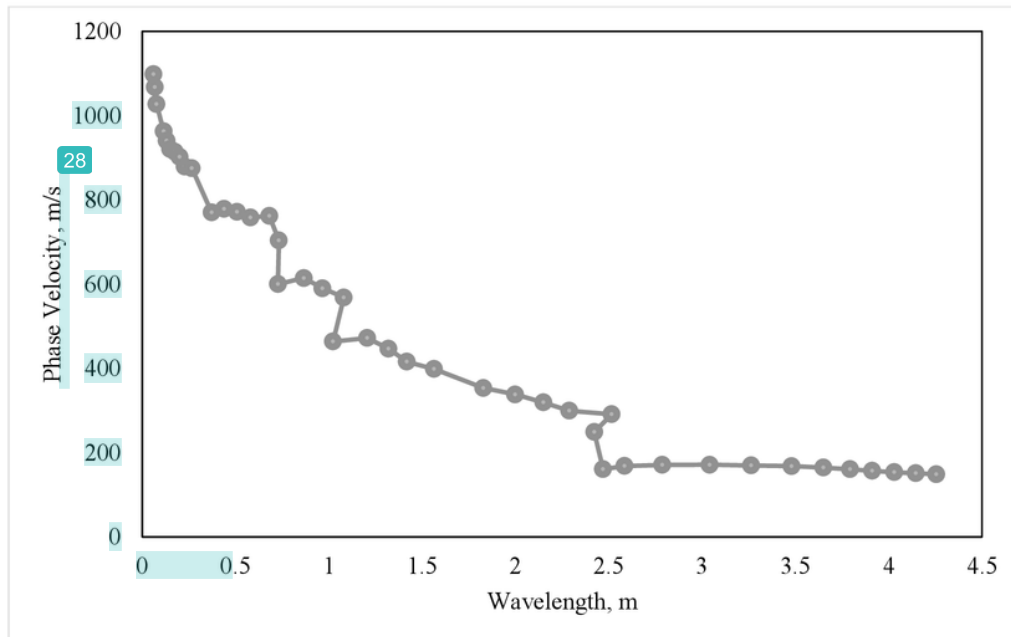
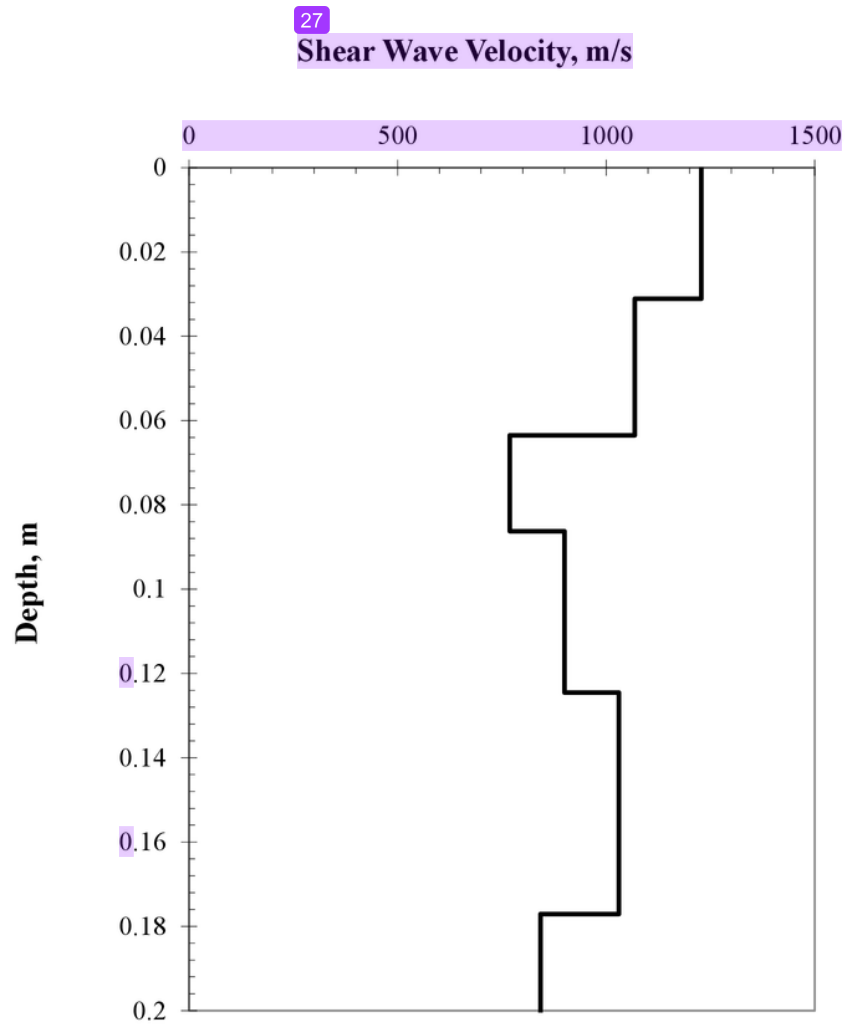


Figure 9. Example of a typical dispersion curve for SASW tests conducted on the Cikampek Purwakarta pavement road, Indonesia showing the variation in wavelength and phase velocity



4

Figure 10. Shear wave velocity profile from inversion of an experimental dispersion curve measured using the SASW test on a national road network in Purwakarta, West Java, Indonesia

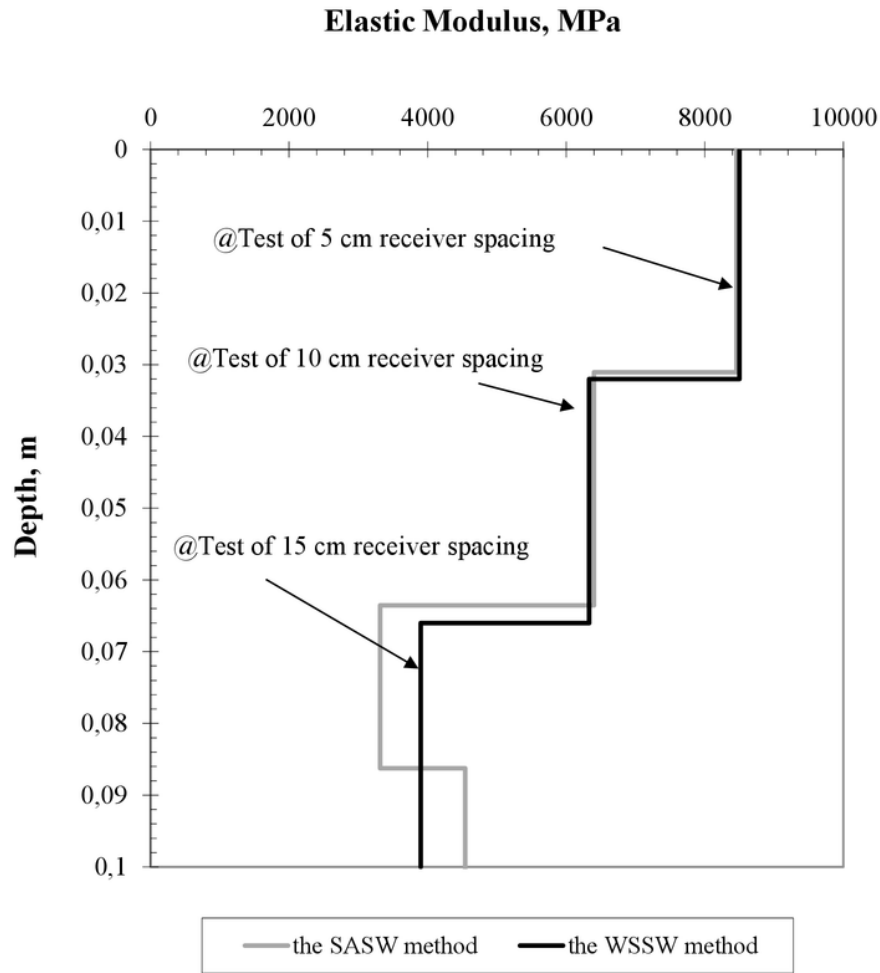


Figure 11. Dynamic elastic modulus of pavement profile obtained using the SASW method in comparison to that of the WSSW method

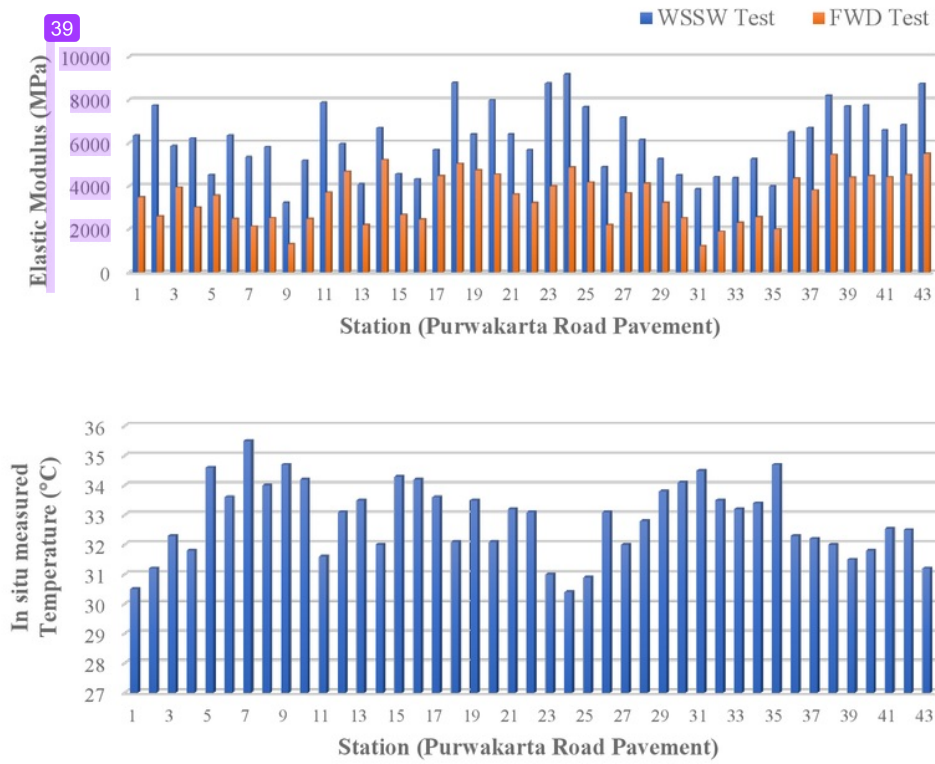
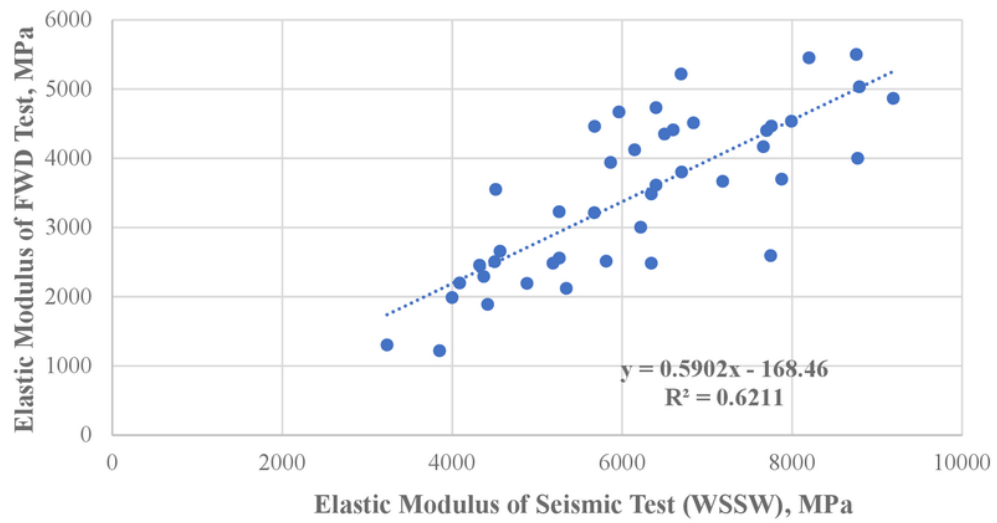


Figure 12. Comparison of elastic modulus of surface layers for a national road in Purwakarta, Indonesia obtained using the SASW and FWD tests



4
Figure 13. Linear regression analysis and data trendline of elastic modulus of surface layers from the WSSW test and FWD test on a national road in Purwakarta, Indonesia

#

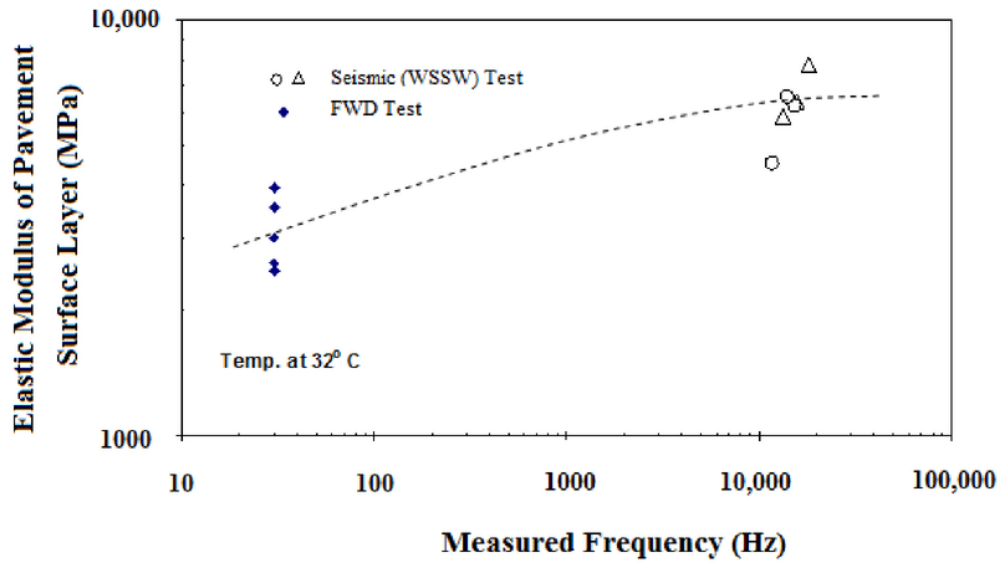
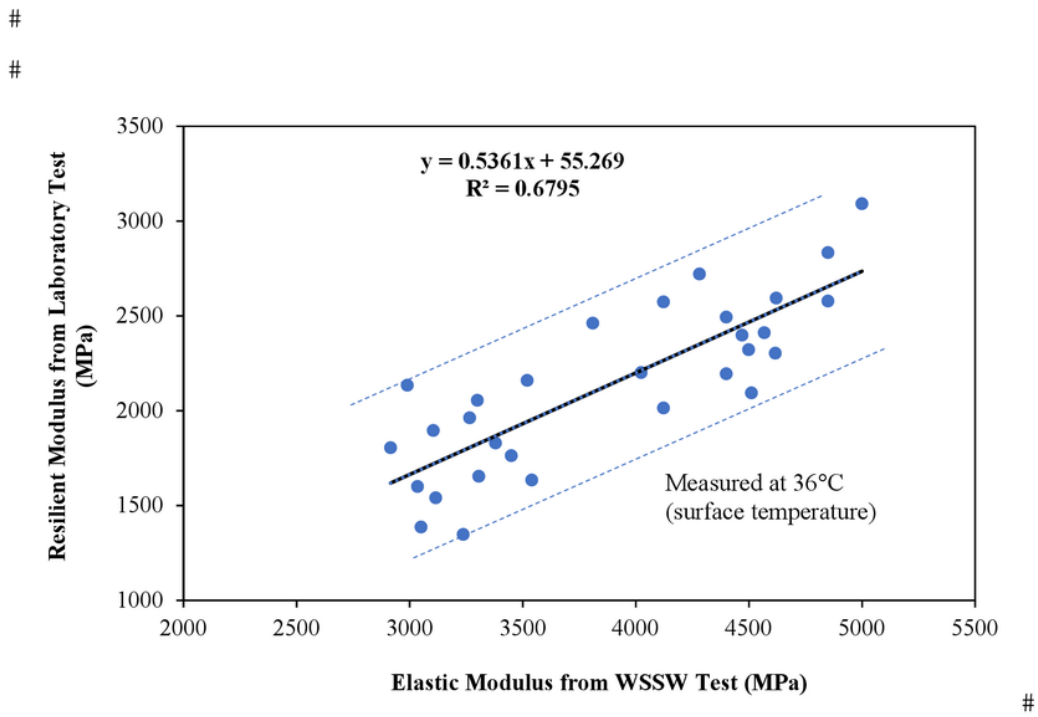


Figure 14. Comparison of the effect of loading frequency on a small strain elastic modulus of an asphalt concrete in Purwakarta, Indonesia obtained from ² FWD and WSSW tests conducted at a temperature of 32° C



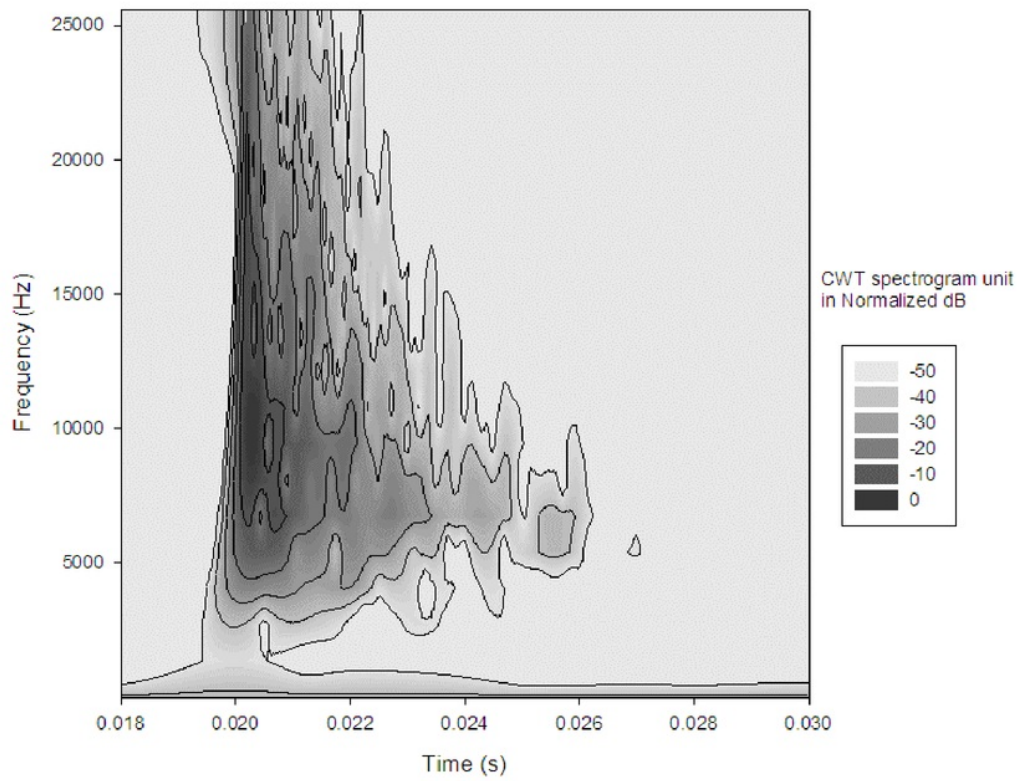
#

6

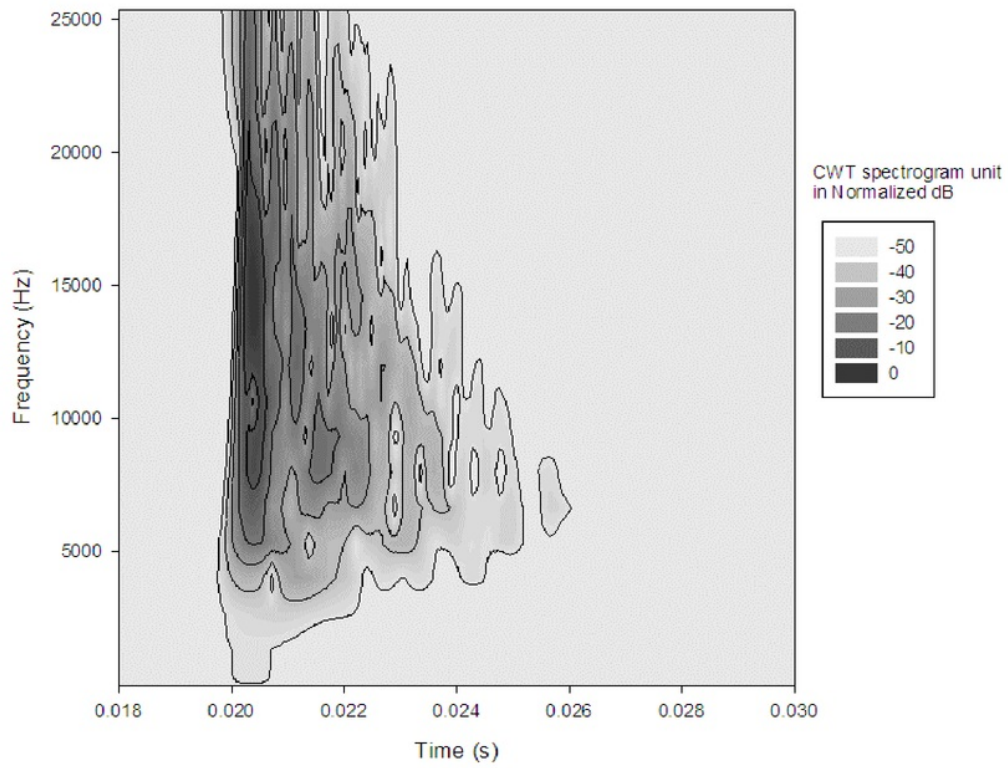
Figure 15. Regression analysis on elastic modulus obtained from the WSSW test and laboratory resilient modulus on road-pavement at the UKM Campus, Malaysia

#

#



(a). CWT Spectrogram for receiver 1



(b). CWT Spectrogram for receiver 2

Figure 17. Time-frequency plot of received signals from field measurement of rigid pavement in Yogyakarta, Indonesia

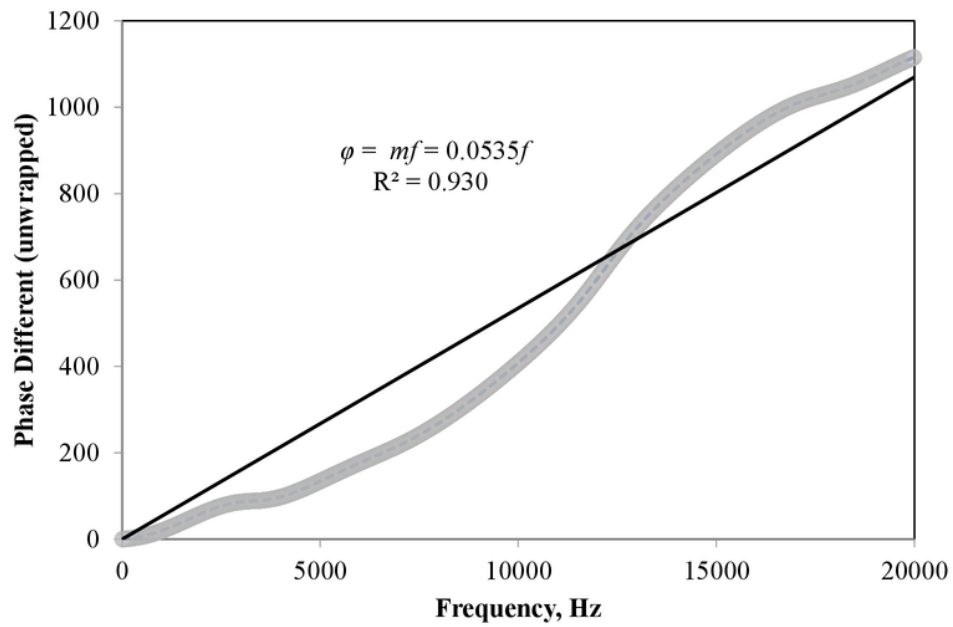


Figure 18. Linear relationship of phase difference and frequency in the unwrapped transfer function for obtaining the slope (m) parameter at rigid pavement site in Yogyakarta, Indonesia

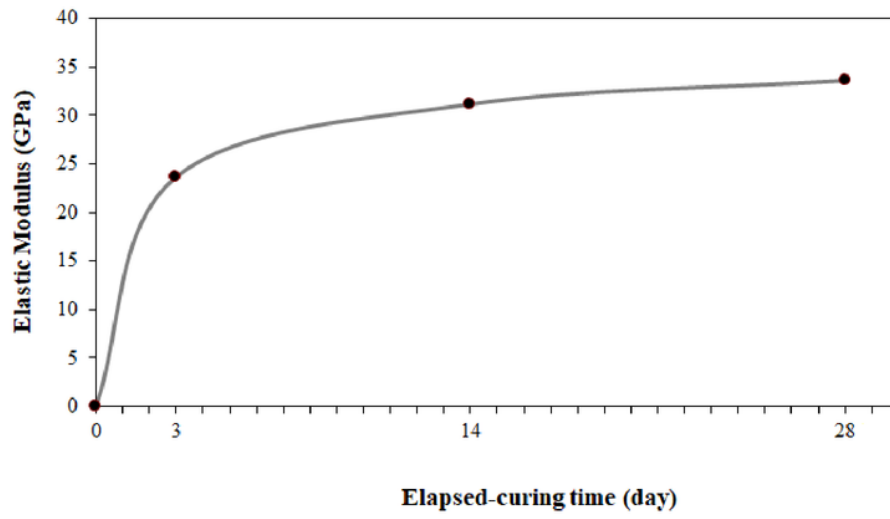
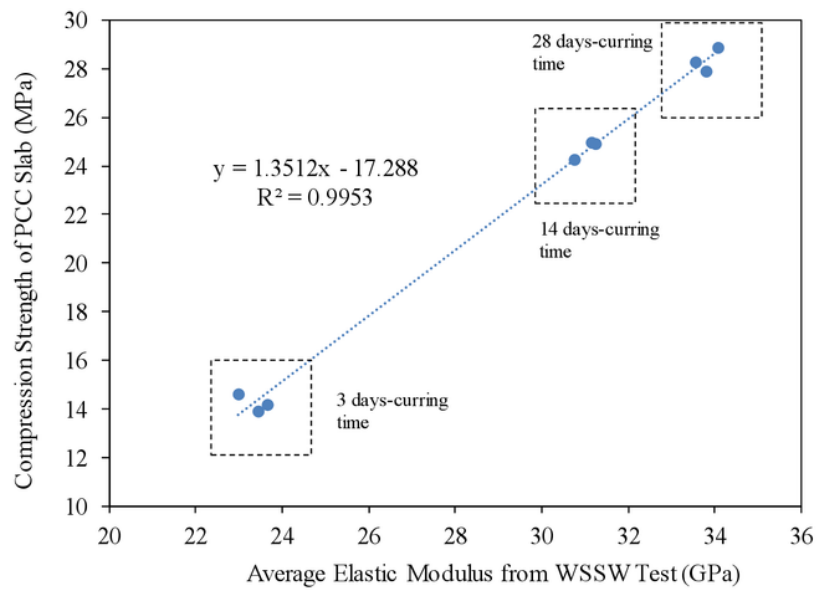


Figure 19. Stiffness monitoring at various elapsed-curing time using the WSSW test on rigid pavement sites



6
Figure 20. Comparison of average elastic modulus obtained through the WSSW test and laboratory compression strength of PCC slabs for rigid pavements with different curing time

Figure Caption List

Figure 1. Experimental set up for WSSW measurement on a pavement structure

Figure 2. Mid-point receiver configuration for WSSW measurement on pavement structure

Figure 3. Typical signals from WSSW measurement on a pavement structure

Figure 4. Time-frequency plot of received signals from WSSW measurement at national road pavement site in Purwakarta, Indonesia

Figure 5. Comparison of raw data and best-fit curve of wrapped transfer function spectrum based on measurements

Figure 6. Coherent function spectrum of received signals from measurement

Figure 7. Linear relationship of phase difference and frequency in the unwrapped transfer function for obtaining the slope (m) parameter at flexible pavement site in Purwakarta, Indonesia

Figure 8. Elastic modulus profile of pavement obtained using the WSSW method for an overlay and existing surface layer of a flexible pavement test site at Purwakarta, Indonesia

Figure 9. Example of a typical dispersion curve for SASW tests conducted on the Cikampek Purwakarta pavement road, Indonesia showing the variation in wavelength and phase velocity

Figure 10. Shear wave velocity profile from inversion of an experimental dispersion curve measured using the SASW test on a national road network in Purwakarta, West Java, Indonesia

Figure 11. Dynamic elastic modulus of pavement profile obtained using the SASW method in comparison to that of the WSSW method

Figure 12. Comparison of elastic modulus of surface layers for a national road in Purwakarta, Indonesia obtained using the SASW and FWD tests

Figure 13. Linear regression analysis and data trendline of elastic modulus of surface layers from the WSSW test and FWD test on a national road in Purwakarta, Indonesia

Figure 14. Comparison of the effect of loading frequency on a small strain elastic modulus of an asphalt concrete in Purwakarta, Indonesia obtained from FWD and WSSW tests conducted at a temperature of 32° C

Figure 15. Regression analysis on elastic modulus obtained from the WSSW test and laboratory resilient modulus on road-pavement at the UKM Campus, Malaysia

Figure 16. Comparison of elastic modulus obtained using the WSSW test and laboratory resilient modulus obtained through the Indirect Tensile Test on existing flexible pavement on the UKM Campus, Malaysia

Figure 17. Time-frequency plot of received signals from field measurement of rigid pavement in Yogyakarta, Indonesia

Figure 18. Linear relationship of phase difference and frequency in the unwrapped transfer function for obtaining the slope (m) parameter at rigid pavement site in Yogyakarta, Indonesia

Figure 19. Stiffness monitoring at various elapsed-curing time using the WSSW test on rigid pavement sites

Figure 20. Comparison of average elastic modulus obtained through the WSSW test and laboratory compression strength of PCC slabs for rigid pavements with different curing time



Click here to access/download
Supplemental Data File²²
GeoMeast_Springer2017.pdf



Response to Reviewer Comments Instructions

Please click on the red comments flag for more information

8	Wavelet Spectrogram Analysis of Surface Wave Technique for In-situ Pavement Stiffness Measurement
---	---------------------------------------------------------------------------------------------------

Manuscript #	Ms. No. MTENG-6490
--------------	--------------------

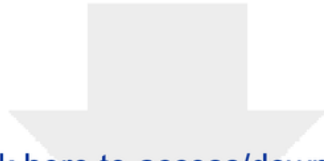
13 The authors wish to thank the editors and reviewers for their time in effort in reviewing our manuscript. We hope the changes listed have made the manuscript suitable for publication and we look forward to your response.

Editor Comments	Author's Response
Your Technical Paper, listed above, has completed a review for publication in ASCE's Journal of Materials in Civil Engineering. The editor has requested that minor revisions be made based on the reviewers' evaluations (shown at the end of this email) and submitted for re-review by 03/02/2018. This revision will only be seen again by the editor and will not undergo the entire review	Authors would like to thank you for the comments from the editor and reviewers. The suggested correction has been made based on the reviewers' evaluation.
Reviewer 2's Comments	Author's Response
The paper is suitable for technical note. However, after addressing following comments. 1. The paper still needs improvement in English and grammar	We would like to thank you for the manuscript review in the English and grammar for improving our manuscript. The correction has been made on the manuscript. An English proofreading was also conducted by professional English proofreader.
2. Figure 14 values look on higher end. Are they realistic particularly at 32 C?	Authors would like to thank you for the comments. We have double check in data and analysis of WSSW test which show that the the elastic modulus of asphaltic materials obtained in the result are re- 33 c. It was also in the acceptable range of elastic modulus for AC materials as reported by Stokoe et al. (1991), Nazarian et al. (1991). In Figure 14, the seismic testing uses the high frequency which produces higher modulus compared to FWD. In addition, the results of elastic modulus from WSSW and compared results from FWD in Figure 14 are also presented in Figure 13 with various temperature observation. We reported the elastic modulus in the y-axis with logarithmic scale.
3. The compression strength of PCC slabs for reported in Figure 20, is not seems to be incorrect. Please check	We would like to thank you for correction on the compressive strength. The correction has been made. The corrected value of compressive strength (in MPa) was reported in

Figure 20.

Reviewer 3's Comments	Author's Response
The comments were properly addressed and the paper is ready to be published.	25 The authors wish to thank the reviewer for their time in effort in reviewing, correcting and giving the feedback on our manuscript.

Thank you again for your time and effort, and for helping us improve the manuscript.

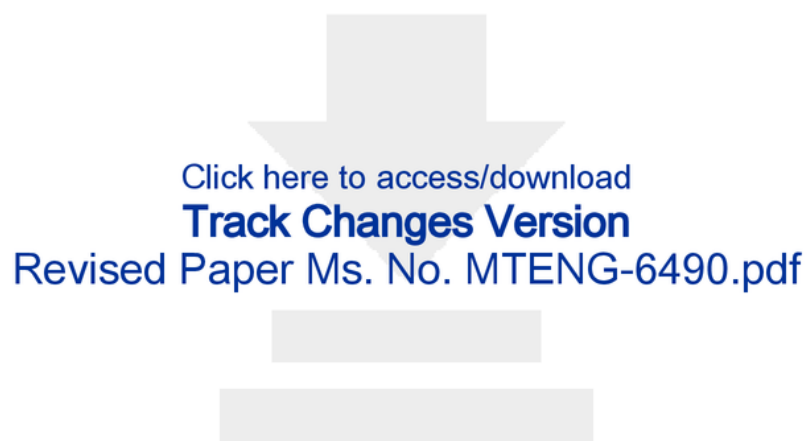


[Click here to access/download](#)

Track Changes Version

[SUCI-D-16-00543_revised6_JMCE ASCE.pdf](#)





13%

SIMILARITY INDEX

PRIMARY SOURCES

- 1** Cimara Fortes Ferreira, Edival Barreto de Magalhães Junior, Barbara Zini. "Optimizing anterior implant esthetics with a vascularized interpositional periosteal connective tissue graft for ridge augmentation: a case report.", *Journal of Oral Implantology*, 2018 162 words — 2%

Crossref
- 2** library.ctr.utexas.edu 102 words — 1%

Internet
- 3** Sri Atmaja P. Rosyidi. "Signal reconstruction of surface waves on SASW measurement using Gaussian Derivative wavelet transform", *Acta Geophysica*, 09/2009 100 words — 1%

Crossref
- 4** Rosyidi, Sri Atmaja P., and Mohd.Raihan Taha. "Coupled Procedure for Elastic Modulus and Damping Ratio Measurement on Pavement Subgrade Structures Using Surface Wave Method", *Contemporary Topics on Testing Modeling and Case Studies of Geomaterials Pavements and Tunnels*, 2011. 90 words — 1%

Crossref
- 5** Rosyidi, Sri Atmaja P.. "Simultaneous in-situ Stiffness and Anomalies Measurement on Pavement Subgrade Using Tomography Surface Waves Technique", *Procedia Engineering*, 2015. 72 words — 1%

Crossref
- 6** Rosyidi, Sri Atmaja P.. "Use of Wavelet Analysis and Filtration on Impulse Response for SASW Measurement in PCC Slab of Pavement Structure", 71 words — 1%

Contemporary Topics on Testing Modeling and Case Studies of Geomaterials Pavements and Tunnels, 2011.

Crossref

-
- 7 docslide.us 63 words — 1%
Internet
-
- 8 www.intechopen.com 48 words — < 1%
Internet
-
- 9 P. Rosyidi, Sri Atmaja, and Mohd. Raihan. 46 words — < 1%
"Wavelet Spectrogram Analysis of Surface Wave
Technique for Dynamic Soil Properties Measurement on Soft
Marine Clay Site", *Seismic Waves - Research and Analysis*, 2012.
Crossref
-
- 10 [Review of Progress in Quantitative Nondestructive Evaluation, 1999.](#) 42 words — < 1%
Crossref
-
- 11 masw.com 39 words — < 1%
Internet
-
- 12 Yusoff, Nur Izzi Md., Sentot Hardwiyono, Norfarah
Nadia Ismail, Mohd Raihan Taha, Sri Atmaja P.
Rosyidi, and Khairul Anuar Mohd Nayan. 35 words — < 1%
"Measurements of the elastic modulus of
pavement subgrade layers using the SASW and FWD test
methods", *The Baltic Journal of Road and Bridge Engineering*,
2015.
Crossref
-
- 13 www.nat-hazards-earth-syst-sci-discuss.net 33 words — < 1%
Internet
-
- 14 Yuan, Jiabei, Jinying Zhu, and Changyoung Kim. 24 words — < 1%
"Comparison of SASW and MASW methods using
MSOR approach – a case study", *International Journal of
Geotechnical Engineering*, 2014.
Crossref
-
- 15 Nazarian, Soheil, and Manuel Celaya. "A Case Study on Quality

Management of Unbound Layers with Seismic Methods", GeoCongress 2006, 2006.

Crossref

19 words — < 1%

16 real.mtak.hu

Internet

19 words — < 1%

17 scholar.lib.vt.edu

Internet

17 words — < 1%

18 Shafabakhsh, Gholamali Tanakizadeh, Amin. "Investigation of loading features effects on resilient modulus of asphalt mixtures using Adaptive Ne", Construction and Building Materials, Feb 1 2015 Issue

Publication

17 words — < 1%

19 www.lsi.uvigo.es

Internet

16 words — < 1%

20 ctis.utep.edu

Internet

16 words — < 1%

21 eprints.whiterose.ac.uk

Internet

15 words — < 1%

22 home.iitk.ac.in

Internet

15 words — < 1%

23 InCIEC 2014, 2015.

Crossref

15 words — < 1%

24 Ryden, Nils, Choon B. Park, Peter Ulriksen, and Richard D. Miller. "Multimodal Approach to Seismic Pavement Testing", Journal of Geotechnical and Geoenvironmental Engineering, 2004.

Crossref

14 words — < 1%

25 Gosu, Vijayalakshmi, Bhola Ram Gurjar, Tian C. Zhang, and Rao Y. Surampalli. "Oxidative Degradation of Quinoline Using Nanoscale Zero-Valent Iron Supported by Granular Activated Carbon", Journal of Environmental Engineering, 2015.

12 words — < 1%

-
- 26 Christopher Phillips. "Evaluation of horizontal homogeneity of geomaterials with the distance analysis of surface waves", *Canadian Geotechnical Journal*, 04/2004
Crossref 12 words — < 1%
-
- 27 amsacta.unibo.it
Internet 11 words — < 1%
-
- 28 www.readbag.com
Internet 11 words — < 1%
-
- 29 dspace.lboro.ac.uk
Internet 10 words — < 1%
-
- 30 portal.research.lu.se
Internet 10 words — < 1%
-
- 31 repository.tudelft.nl
Internet 9 words — < 1%
-
- 32 www-geo.phys.ualberta.ca
Internet 9 words — < 1%
-
- 33 theses.bham.ac.uk
Internet 9 words — < 1%
-
- 34 Sri Atmaja P. Rosyidi, Mohd. Raihan. "Chapter 7 Wavelet Spectrogram Analysis of Surface Wave Technique for Dynamic Soil Properties Measurement on Soft Marine Clay Site", *InTech*, 2012
Crossref 9 words — < 1%
-
- 35 repositories.lib.utexas.edu
Internet 9 words — < 1%
-
- 36 atmaja.staff.umy.ac.id
Internet 9 words — < 1%
-
- 37 Hunaidi, O.. "Evolution-based genetic algorithms for analysis of

non-destructive surface wave tests on pavements", 9 words — < 1 %
NDT and E International, 199808
Crossref

38 Luke, Barbara A., and Kenneth H. Stokoe II. 8 words — < 1 %
"Application of SASW Method Underwater", Journal
of Geotechnical and Geoenvironmental Engineering, 1998.
Crossref

39 etd.auburn.edu 8 words — < 1 %
Internet

40 Ali Zomorodian, S.M.. "Inversion of SASW 8 words — < 1 %
dispersion curves based on maximum flexibility
coefficients in the wave number domain", Soil Dynamics and
Earthquake Engineering, 200608
Crossref

41 Bjurstrom, Henrik Gudmarsson, Anders Ryd. "Field 8 words — < 1 %
and laboratory stress-wave measurements of
asphalt concrete.(Report)(Abstract)", Construction and Building
Materials, Nov 15 2016 Issue
Publication

42 dalspace.library.dal.ca 8 words — < 1 %
Internet

43 "Numerical Study on Guided Wave Propagation in 8 words — < 1 %
Wood Utility Poles: Finite Element Modelling and
Parametric Sensitivity Analysis", Applied Sciences, 2017
Crossref

44 D S Kim, H C Park. "Evaluation of ground 8 words — < 1 %
densification using spectral analysis of surface
waves (SASW) and resonant column (RC) tests",
Canadian Geotechnical Journal, 1999
Crossref

45 Xue, Wenjing, Linbing Wang, Dong Wang, and 8 words — < 1 %
Christian Druta. "Pavement Health Monitoring
System Based on An Embedded Sensing Network", Journal of
Materials in Civil Engineering, 2013.

-
- 46 www.scribd.com
Internet 8 words — < 1%
-
- 47 66.180.169.221
Internet 8 words — < 1%
-
- 48 www.coursehero.com
Internet 8 words — < 1%
-
- 49 rrijogja.co.id
Internet 8 words — < 1%
-
- 50 Shanqiang Li, Feng Liu, Xinquan Xu, Hao Li.
"Inertial point influencing factors analysis of the
flexible pavement structure under the moving load", AIP
Publishing, 2017
Crossref 7 words — < 1%
-
- 51 Margherita Maraschini. "A new misfit function for
multimodal inversion of surface waves",
Geophysics, 2010
Crossref 7 words — < 1%
-
- 52 Cho, Y.S.. "Spectral analysis of surface wave
response of multi-layer thin cement mortar slab
structures with finite thickness", NDT and E International, 200103
Crossref 6 words — < 1%
-
- 53 Kim, D.S.. "Evaluation of density in layer
compaction using SASW method", Soil Dynamics
and Earthquake Engineering, 200101
Crossref 6 words — < 1%
-
- 54 "Geotechnics for Natural and Engineered
Sustainable Technologies", Springer Nature, 2018
Crossref 6 words — < 1%
-

EXCLUDE BIBLIOGRAPHY ON